FACULTY OF SCIENCE
UNIVERSITY OF COPENHAGEN

Topological superconductivity and Majorana fermions in 2D lattice models

Hano Omar Mohammad Sura

Niels Bohr Institute
University of Copenhagen
Blegdamsvej 17, DK-2100, Copenhagen, Denmark

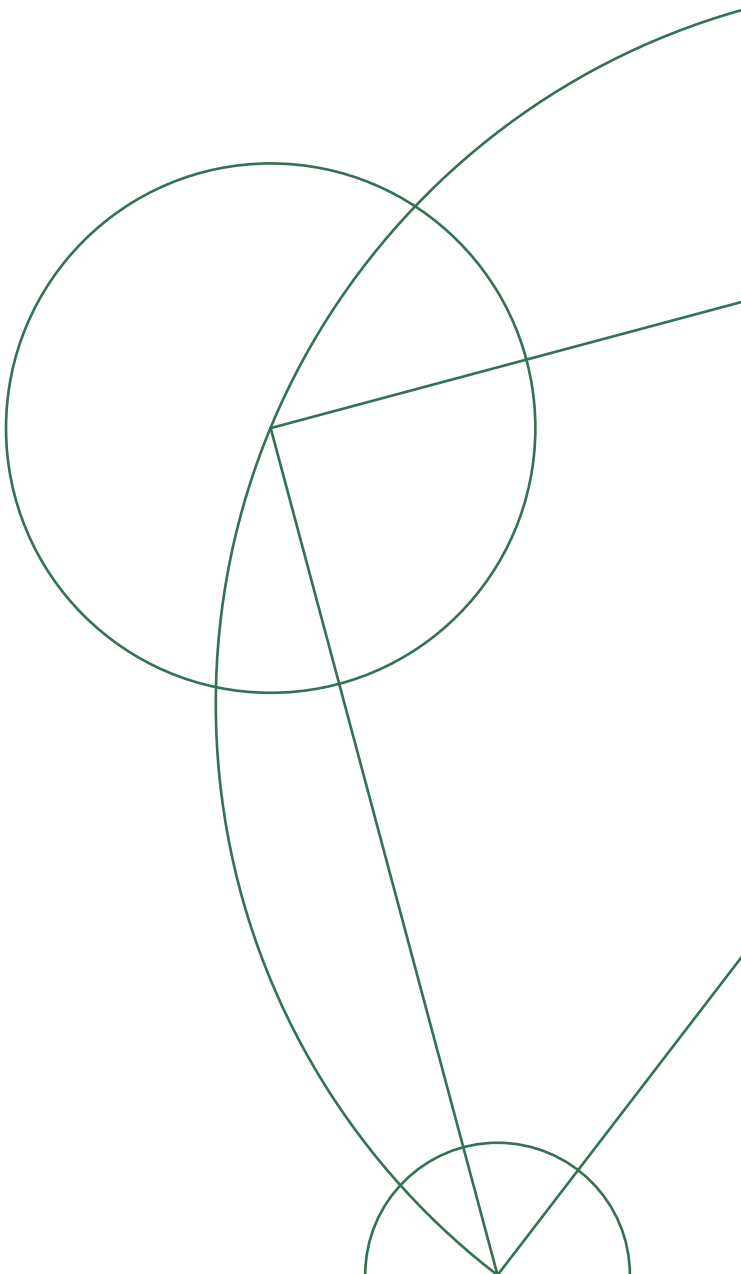

Bachelor's thesis in Physics

Advisor: Brian M. Andersen

Dated: July 9, 2017

Abstract

In this thesis the main objective is to numerically explore the topological phases of a 2D square lattice model, which includes s-wave superconductivity, Rashba-spin orbit coupling, an extern magnetic field and nearest-neighbor hopping. The numerical calulations are based on rewriting the original Hamiltonian in the Bogoliubov-de-Gennes form, and it is argued that zero-energy eigenstates of the Hamiltonian are Majorana fermions. The symmetry class of the bulk system is found to be D, which in 2D systems, based on the periodic table for topological insulators and superconductors, means that topologically non-trivial phases exist.

Considering a semi-periodic system it is found that in the non-trivial phases, the lowest-energy states are confined to the edges of the system. The dispersing smallest energy states are chiral, while the actual zero-energy states, the Majorana states, are confined to both edges of the system. The local density of states (LDOS) is found near the edges and in the bulk of the system in both a trivial and non-trivial phase of the system. Comparing these, it is possible to discern the trivial and non-trivial phase by the appearance of finite state density at $E = 0$.

Placing a vortex-like phase with winding number $m = 1$ in a system with completely open boundaries, zero-energy states also appear. These states are split up, one confined to the edges of the system and one to the core of the vortex, when choosing a specific basis in the zero-energy states. A comparison between the LDOS in the system in the trivial and non-trivial phases is made, and the same qualitiative difference is found as in the semi-periodic system.

Finally, an on-site potential impurity is placed in a system with periodic boundaries, to explore whether this will induce zero-energy states in the system. These did not induce zero-energy states, and therefore no qualitative difference could be found between the topologically trivial and non-trivial phases.

Contents

1 Introduction

Since the discovery of the first superconductor in 1911 by Heike Kamerlingh Onnes, these types of materials have been studied with great interest and many different have been found. The publishing of the first microscopic theory of superconductivity by Bardeen, Cooper and Schrieffer in 1957 was a great step towards understanding this phenomenon, but not all observed superconductors are explainable through their theory. Recently, more interest has been around p-wave superconductors and the topological properties of these. Especially interesting is the theoretically predicted emergence of Majorana fermions in the so called topologically non-trivial phases of the superconductors, as these are particles that have not been observed outside of condensed matter systems and might be used as components in a quantum computer.

Topology in condensed matter physics is the study of properties of systems that can continuously be deformed into one another. Such systems are called topologically equivalent, and share so-called topological invariants. Furthermore, one can classify a system into the so called trivial and non-trivial topologial phases. In a non-trivial topological phase, materials share peculiar properties, for example the appearance of zero-energy states confined to the edges of the system. The quantum Hall effect is an example of a phenomenon of non-trivial topology, and is associated with chiral edge states.

This thesis explores a type of s-wave superconductor, rather than a p-wave superconductor, which shares some of the same properties as the p-wave superconductor. More specifically, we consider an s-wave superconductor in which the electrons are subject to an external magnetic field and Rashba spin- orbit coupling. This model exhibits symmetries that imply existence of non-trivial topological phases. We will explore these phases and the occurence of edge states in 1D and 2D models using the Bogoliubov-de-Gennes method, and argue why the edge states that appear in a non-trivial phase are Majorana fermions. A vortex-like phase is added to the superconducting gap in a finite 2D system, and the implicitations for the appearance of zero energy states are explored. In particular we discuss the observation of Majorana states being divided into one on the edge of the system and one around the vortex core.
Finally we also explore whether an on-site potential impurity induces zero-energy states in a non-trivial phase of the system.

A brief introduction to the second quantization formalism is given in appendix A, an introduction to the BCS theory of superconductivity is given in appendix B and a short explanation for the Rashba spin-orbit coupling and its second quantized form is given in appendix C, which also serves as an example of writing operators in second quantization. In appendix J an example of the calculations made in the Matlab scripts has been added, as well as a link to the most relevant scripts made during the project.

2 Topology in condensed matter physics

Topology in mathematics is loosely speaking concerned with classifying shapes, or spaces. One classifies a set of spaces to one equivalence class if they can be continuously deformed into one another, that is, without tearing or gluing the space. One can characterize a space by its Euler characteristic

$$\chi = \frac{1}{2\pi}\int GdS = (2-2h), \tag{2.1}$$

where G is the Gaussian curvature. Here h is the number of "holes" in the space. The canonical example is the donut and the cup shapes, that are topologically equivalent but are inequivalent to, say, a sphere. Thus they belong to different equivalence classes. It is worth mentioning that also the space in which the shape is embedded influences the equivalence class.[2]
In condensed matter systems one can also classify certain systems, i.e. Hamiltonians, as belonging to the same equivalence class. That is, one can continuously deform one Hamiltonian into another. In these systems continuous deformation means that one transforms the Hamiltonian without letting one of the eigenenergies become degenerate. One example of a topological invariant is the first Chern number defined as

$$C = \frac{1}{2\pi}\int_S \mathbf{B}\cdot d\mathbf{a}, \tag{2.2}$$

where $\mathbf{B}$ is the so called Berry curvature and the integral is over the first Brillouin zone of a 2D system.

2.1 The Berry phase

The Chern number is defined through the Berry phase, a special case of the geometric phase. A thorough study of this is done in appendix D.
The Berry phase is a geometric phase acquired by a state when it moves adiabatically through a closed curve in the parameter space of the Hamiltonian,

$$\gamma_n(t) = i \oint \langle \psi_n | \frac{\partial \psi_n}{\partial P_i} \rangle \, d\mathbf{P}. \tag{2.3}$$

Since the endpoints of the curve the state moves through in parameter space are the same, this phase cannot be set to 0 by a simply phase change, making the Berry phase a physical observable. Through this phase one can also define the Berry curvature,

$$\mathbf{B}_n = i \sum_{m \neq n} \frac{\langle \psi_n | \nabla H | \psi_m \rangle \times \langle \psi_m | \nabla H | \psi_n \rangle}{(E_n - E_m)^2}, \tag{2.4}$$

which has the same function in the definition of Chern number as the Gaussian curvature has when defining the Euler characteristic. It is clear that the Berry curvature diverges if an eigenenergy is degenerate. A diverging Berry curvature is what results in a non-zero Chern number. This is the reason why, when studying condensed matter systems, the closing of gap in the energy spectrum leads to a possibly non-zero Chern number.

2.2 The Chern number

Using the Berry curvature one can define the first Chern number through (2.2). This number is called a type $\mathbb{Z}$ topological invariant. Whenever it is non-zero, the system is in a topologically non-trivial phase. Thus, when studying such systems, the closing of gaps in the energy spectrum, become important in determining the topological phase of the system.
The Chern number is the topological invariant in many different systems, and is the relevant invariant in the 2D system introduced in section 3. An example of another system where it is relevant is a system exhibiting integer quantum Hall effect (IQHE), where it is a calculation of the filling factor [6].
In this thesis we only refer to it as an indicator of the topological phase of the systems under consideration.

2.3 Symmetries and topological classes

One can classify physical systems (/models/Hamiltonians) into groups according to whether they have a topologically trivial phase. We classify a system according to whether operators exist where[5],

$$\mathcal{T} \quad \text{is anti-unitary and} \quad \mathcal{T}^\dagger \mathcal{H}(\mathbf{r}, \mathbf{k}) \mathcal{T} = \mathcal{H}(\mathbf{r}, -\mathbf{k}), \tag{2.5}$$

$$\mathcal{P} \quad \text{is anti-unitary and} \quad \mathcal{P}^\dagger \mathcal{H}(\mathbf{r}, \mathbf{k}) \mathcal{P} = -\mathcal{H}(\mathbf{r}, -\mathbf{k}), \tag{2.6}$$

$$\mathcal{C} \quad \text{is unitary and} \quad \mathcal{C}^\dagger \mathcal{H}(\mathbf{r}, \mathbf{k}) \mathcal{C} = -\mathcal{H}(\mathbf{r}, \mathbf{k}), \tag{2.7}$$

and an anti-unitary operator has the property that, when using it on a complex number,

$$\mathcal{T}^\dagger Z \mathcal{T} = U^\dagger Z^* U, \tag{2.8}$$

where U is a unitary operator. That is, an anti-unitary operator can be written as a combination of the complex conjugation operator, $\mathcal{K}$, and a unitary operator. We refer to a system where (2.5) is fulfilled as time-reversal symmetric, one where (2.6) is fulfilled as particle-hole symmetric and one where (2.7) as chiral symmetric. Generally

$$\mathcal{T}^2 = \pm I, \;\; \mathcal{P}^2 = \pm I, \;\; \mathcal{C}^2 = I, \tag{2.9}$$

which is a result of the anti-unitarity of the first two operators and the unitarity of the last. Now, the operator $\mathcal{C}$ can be written as a product of the two anti-unitary operators since, if they exist,

$$\mathcal{T}^\dagger \mathcal{P}^\dagger \mathcal{H} \mathcal{P} \mathcal{T} = \mathcal{P}^\dagger \mathcal{T}^\dagger \mathcal{H} \mathcal{T} \mathcal{P} = -\mathcal{H}, \tag{2.10}$$

$$(\mathcal{T}\mathcal{P})(\mathcal{T}\mathcal{P})^\dagger = (U_\mathcal{T} U_\mathcal{P}^*)(U_\mathcal{T} U_\mathcal{P}^*)^\dagger = I \tag{2.11}$$

establishing that the product of the two operators fulfill the same requirement as $\mathcal{C}$ and is unitary. Thus, if two of the three operators exist so does the third, which means there are 10 possible operator existence

Class	Symmetry			d				
	$\mathcal{T}$	$\mathcal{P}$	$\mathcal{C}$	1	2	3	4	...
A	0	0	0	0	$\mathbb{Z}$	0	$\mathbb{Z}$	...
AIII	0	0	1	$\mathbb{Z}$	0	$\mathbb{Z}$	0	...
AI	1	0	0	0	0	0	$\mathbb{Z}$	...
BDI	1	1	1	$\mathbb{Z}$	0	0	0	...
D	0	1	0	$\mathbb{Z}_2$	$\mathbb{Z}$	0	0	...
DIII	-1	1	1	$\mathbb{Z}_2$	$\mathbb{Z}_2$	$\mathbb{Z}$	0	...
AII	-1	0	0	0	$\mathbb{Z}_2$	$\mathbb{Z}_2$	$\mathbb{Z}$	...
CII	-1	-1	1	$\mathbb{Z}$	0	$\mathbb{Z}_2$	$\mathbb{Z}_2$	...
C	0	-1	0	0	$\mathbb{Z}$	0	$\mathbb{Z}_2$	...
CI	1	-1	1	0	0	$\mathbb{Z}$	0	...

Table 1: Topological classification based on system dimension, d, and existing symmetries. Table taken from [7].

combinations. Table 1 shows for which combinations of existing operators there exists a topologically non-trivial phase of a system, and which type of invariant is associated with the non-trivial phase. $\mathbb{Z}$ and $\mathbb{Z}_2$ refer to the type of topological invariant the system can have. We will not delve into the different kinds of invariants.

3 Methods

The Hamiltonian generally considered in this thesis is of the form:

$$\begin{aligned} H = &-t \sum_{\langle i,j\rangle,\sigma} c^\dagger_{i,\sigma} c_{j,\sigma} - \mu \sum_{i,\sigma} c^\dagger_{i,\sigma} c_{i,\sigma} \\ &+ E_{so} \sum_{j\delta_x\delta_y} \sum_{\sigma,\sigma'} i \left(c^\dagger_{j\sigma} \sigma^{(x)}_{\sigma,\sigma'} c_{j+\delta_y\sigma'} - c^\dagger_{j\sigma} \sigma^{(y)}_{\sigma,\sigma'} c_{j+\delta_x\sigma'} + h.c. \right) \\ &- \gamma B \sum_{i,\sigma,\sigma'} \sigma^{(z)}_{\sigma,\sigma'} c^\dagger_{i\sigma} c_{i\sigma'} + \sum_i \Delta c^\dagger_{i\uparrow} c^\dagger_{i\downarrow} + \Delta^* c_{i\downarrow} c_{i\uparrow}, \end{aligned} \tag{3.1}$$

describing the electrons of a 2D square lattice crystal. The first term describes tight-binding hopping between nearest neighbors, the second term the chemical potential, the third the so called Rashba spin-orbit coupling characterized by the parameter E_{so}, the fourth the Zeeman effect due to a perpendicular magnetic field and the fifth s-wave superconductivity. δ_x and δ_y are the lattice spacing in the x- and y-directions. The $\sigma_{\sigma,\sigma'}$ included refer to the entries of the Pauli matrices, with $\sigma_{\uparrow,\uparrow} = \sigma_{1,1}$. The tight binding term includes only nearest neighbor hoppings. The sums are over crystal sites, and we assume a square crystal with N sites on each edge, resulting in N^2 sites. This model will be used to study crystals with periodic, semi-periodic and open boundaries.

3.1 Bogoliubov-de-Gennes formalism

To study this type of system one employs the so called Bogoliubov-de-Gennes transformation. The central idea is to not only consider the effect on electrons but also on absence of holes in the system. The following illustrates the idea.
Consider the first term in (3.1),

$$-t \sum_{\langle i,j\rangle,\sigma} c^\dagger_{i,\sigma} c_{j,\sigma} = -\frac{t}{2} \sum_{\langle i,j\rangle,\sigma} \left(c^\dagger_{i,\sigma} c_{j,\sigma} + 1 - c_{i,\sigma} c^\dagger_{j,\sigma} \right), \tag{3.2}$$

where we used the fermionic anticommutation relations. We thus obtain a term in the Hamiltonian in which the electron number is on equal footing with the "absence" of the number of holes. This operation does not give us a new Hamiltonian but simply "describes the system twice", once for electrons and once for the absence of holes.

Doing the same thing in every term of (3.1) one can write it as

$$H = \begin{pmatrix} c_{i\uparrow}^\dagger & c_{i\downarrow}^\dagger & c_{i\uparrow} & c_{i\downarrow} \end{pmatrix} \begin{pmatrix} \widehat{N} & \widehat{\Delta} \\ -\widehat{\Delta}^* & -\widehat{N}^T \end{pmatrix} \begin{pmatrix} c_{i\uparrow} \\ c_{i\downarrow} \\ c_{i\uparrow}^\dagger \\ c_{i\downarrow}^\dagger \end{pmatrix} \tag{3.3}$$

$$= \begin{pmatrix} c_{i\uparrow}^\dagger & c_{i\downarrow}^\dagger & c_{i\uparrow} & c_{i\downarrow} \end{pmatrix} \mathcal{H} \begin{pmatrix} c_{i\uparrow} \\ c_{i\downarrow} \\ c_{i\uparrow}^\dagger \\ c_{i\downarrow}^\dagger \end{pmatrix}, \tag{3.4}$$

where the i subscript on the vector entries run over all N^2 sites and each entry in the matrix is an $2N^2$-by-$2N^2$ matrix by itself. Symbolically we write

$$\widehat{N} = \left(\begin{array}{c|c} N_{-(t+\mu)} & N_{so} \\ \hline (N_{so})^* & N_{-(t+\mu)} \end{array} \right) \tag{3.5}$$

$$\widehat{\Delta} = \left(\begin{array}{c|c} 0 & \Delta \\ \hline -\Delta & 0 \end{array} \right), \tag{3.6}$$

emphasizing that each block in these submatrices are themselves N^2-by-N^2 matrices.
The purpose of this construction is to arrive at a form of the Hamiltonian, where it can be diagonalized. Defining a unitary matrix such that

$$U^\dagger \mathcal{H} U = \mathcal{D}, \tag{3.7}$$

where $\mathcal{D}$ is diagonal, we arrive at the form of the Hamiltonian

$$H = \begin{pmatrix} \gamma_{n\uparrow}^{\dagger(-E)} & \gamma_{n\downarrow}^{\dagger(-E)} & \gamma_{n\downarrow}^{\dagger(E)} & \gamma_{n\uparrow}^{\dagger(E)} \end{pmatrix} \mathcal{D} \begin{pmatrix} \gamma_{n\uparrow}^{(-E)} \\ \gamma_{n\downarrow}^{(-E)} \\ \gamma_{n\uparrow}^{(E)} \\ \gamma_{n\downarrow}^{(E)} \end{pmatrix}, \tag{3.8}$$

where the new quasiparticle operators are defined by:

$$\begin{pmatrix} \gamma_{n\uparrow}^{\dagger(-E)} & \gamma_{n\downarrow}^{\dagger(-E)} & \gamma_{n\downarrow}^{\dagger(E)} & \gamma_{n\uparrow}^{\dagger(E)} \end{pmatrix} = \begin{pmatrix} c_{i\uparrow}^\dagger & c_{i\downarrow}^\dagger & c_{i\downarrow} & c_{i\uparrow} \end{pmatrix} U \tag{3.9}$$

$$\begin{pmatrix} \gamma_{n\uparrow}^{(-E)} \\ \gamma_{n\downarrow}^{(-E)} \\ \gamma_{n\downarrow}^{(E)} \\ \gamma_{n\uparrow}^{(E)} \end{pmatrix} = U^\dagger \begin{pmatrix} c_{i\uparrow} \\ c_{i\downarrow} \\ c_{i\downarrow}^\dagger \\ c_{i\uparrow}^\dagger \end{pmatrix}. \tag{3.10}$$

Before we write the final, simple expression of the Hamiltonian, there is a point to be made about the matrix $\mathcal{D}$, which also clarifies the γ-operators superscripts. In our definition of U, $\mathcal{D}$ can be seperated into two equally sized matrices,

$$\mathcal{D} = \left(\begin{array}{cc|cc} -E_\uparrow & 0 & \multicolumn{2}{c}{0} \\ 0 & -E_\downarrow & & \\ \hline \multicolumn{2}{c|}{0} & E'_\downarrow & 0 \\ & & 0 & E'_\uparrow \end{array} \right), \tag{3.11}$$

where the $'$ denotes mirroring such that $E_\uparrow^{1,1} = (E'_\uparrow)^{N^2,N^2}$. Here every entry in the matrices E_σ, E'_σ are positive. Thus the Hamiltonian finally can be written as,

$$H = \sum_n -E_{n\uparrow}\gamma_{n\uparrow}^{\dagger(-E)}\gamma_{n\uparrow}^{(-E)} - E_{n\downarrow}\gamma_{n\downarrow}^{\dagger(-E)}\gamma_{n\downarrow}^{(-E)} + E'_{n\downarrow}\gamma_{n\downarrow}^{\dagger(E)}\gamma_{n\downarrow}^{(E)} + E'_{n\uparrow}\gamma_{n\uparrow}^{\dagger(E)}\gamma_{n\uparrow}^{(E)}. \tag{3.12}$$

3.2 Self-consistency

To obtain the eigenstates of $\mathcal{H}$ (that is the coloumns in U) and thus those of H, we must guess some initial values for the parameters μ and Δ, since the Hamiltonian depends on these parameters. But we also know that,

$$n_i = n_{i\uparrow} + n_{i\downarrow} = \langle c^\dagger_{i\uparrow} c_{i\uparrow}\rangle + \langle c^\dagger_{i\downarrow} c_{i\downarrow}\rangle \tag{3.13}$$

$$\Delta_i = -V_{eff}\,\langle c_{i\downarrow} c_{i\uparrow}\rangle\,, \tag{3.14}$$

where the first equation is simply the electron density expectation value, and the second equation can be derived from the definition of the energy gap in eq. (B.6). Now, using eq. (3.9) and (3.10), we can write the electron operators as linear combinations of quasiparticle operators. But this means that once we know the eigenvectors of $\mathcal{H}$ we can find Δ_i^{BdG}, and if $\Delta_i^{\mathrm{Guess}} \neq \Delta_i^{\mathrm{BdG}}$, we use this new value to recalculate the Hamiltonian. One will, after some iterations, find that the value converges. In practice we demand that $||\Delta_i^{\mathrm{Guess}}| - |\Delta_i^{\mathrm{BdG}}|| < \epsilon$ for some fixed number ϵ.
In the following we will use the following notation for the entries of U, where superscripts refer to coloumns and subscripts rows. The electron operators can be written as:

$$\begin{aligned} U^n_i &= u^n_{i\uparrow} \\ U^n_{i+N^2} &= u^n_{i\downarrow} \qquad \text{for} \qquad i = 1, ..., N^2 \\ U^n_{i+2N^2} &= v^n_{i\uparrow} \qquad \text{and} \qquad n = 1, ..., 4N^2 \\ U^n_{i+3N^2} &= v^n_{i\downarrow} \end{aligned}$$

$$c^\dagger_{i\uparrow} = \sum_n u^{*n}_{i\uparrow}\gamma^{\dagger(-E)}_{n\uparrow} + u^{*n+N^2}_{i\uparrow}\gamma^{\dagger(-E)}_{n\downarrow} + u^{*n+2N^2}_{i\uparrow}\gamma^{\dagger(E)}_{n\downarrow} + u^{*n+3N^2}_{i\uparrow}\gamma^{\dagger(E)}_{n\uparrow}, \tag{3.15}$$

$$c^\dagger_{i\downarrow} = \sum_n u^{*n}_{i\downarrow}\gamma^{\dagger(-E)}_{n\uparrow} + u^{*n+N^2}_{i\downarrow}\gamma^{\dagger(-E)}_{n\downarrow} + u^{*n+2N^2}_{i\downarrow}\gamma^{\dagger(E)}_{n\downarrow} + u^{*n+3N^2}_{i\downarrow}\gamma^{\dagger(E)}_{n\uparrow}, \tag{3.16}$$

$$c_{i\uparrow} = \sum_n u^{n}_{i\uparrow}\gamma^{(-E)}_{n\uparrow} + u^{n+N^2}_{i\uparrow}\gamma^{(-E)}_{n\downarrow} + u^{n+2N^2}_{i\uparrow}\gamma^{(E)}_{n\downarrow} + u^{n+3N^2}_{i\uparrow}\gamma^{(E)}_{n\uparrow}, \tag{3.17}$$

$$c_{i\downarrow} = \sum_n u^{n}_{i\downarrow}\gamma^{(-E)}_{n\uparrow} + u^{n+N^2}_{i\downarrow}\gamma^{(-E)}_{n\downarrow} + u^{n+2N^2}_{i\downarrow}\gamma^{(E)}_{n\downarrow} + u^{n+3N^2}_{i\downarrow}\gamma^{(E)}_{n\uparrow}. \tag{3.18}$$

The quasiparticles are themselves linear combinations of the electronic operators, and their operators can be shown to obey the fermionic anticommutation rules. They are thus fermions and behave as such. Specifically,

$$\langle \gamma^\dagger_{n\sigma}\gamma_{n'\sigma'}\rangle = \delta_{nn'}\delta_{\sigma\sigma'} f(E_{n\sigma}), \tag{3.19}$$

$$\langle \gamma_{n\sigma}\gamma^\dagger_{n'\sigma'}\rangle = \delta_{nn'}\delta_{\sigma\sigma'}(1 - f(E_{n\sigma})), \tag{3.20}$$

$$\langle \gamma_{n\sigma}\gamma_{n'\sigma'}\rangle = \langle \gamma^\dagger_{n\sigma}\gamma^\dagger_{n'\sigma'}\rangle = 0, \tag{3.21}$$

where $f(x)$ is the Fermi-Dirac distribution. With this in mind one can find the following expectation values for the electron density,

$$n_{i\sigma} = \sum_n |u^n_{i\sigma}|^2 f(-E_{n\uparrow}) + |u^{n+N^2}_{i\sigma}|^2 f(-E_{n\downarrow}) + |u^{n+2N^2}_{i\sigma}|^2 f(E'_{n\downarrow}) + |u^{n+3N^2}_{i\sigma}|^2 f(E'_{n\uparrow}). \tag{3.22}$$

For calculating the superconducting gap there is one more step. Observe the seemingly ambiguous way of calculating the electron operators from (3.9) and (3.10). From these two equations, one could just as well have written,

$$c_{i\uparrow} = \sum_n v^{*n}_{i\uparrow}\gamma^{\dagger(-E)}_{n\uparrow} + v^{*n+N^2}_{i\uparrow}\gamma^{\dagger(-E)}_{n\downarrow} + v^{*n+2N^2}_{i\uparrow}\gamma^{\dagger(E)}_{n\downarrow} + v^{*n+3N^2}_{i\uparrow}\gamma^{\dagger(E)}_{n\uparrow}, \tag{3.23}$$

$$c_{i\downarrow} = \sum_n v^{*n}_{i\downarrow}\gamma^{\dagger(-E)}_{n\uparrow} + v^{*n+N^2}_{i\downarrow}\gamma^{\dagger(-E)}_{n\downarrow} + v^{*n+2N^2}_{i\downarrow}\gamma^{\dagger(E)}_{n\downarrow} + v^{*n+3N^2}_{i\downarrow}\gamma^{\dagger(E)}_{n\uparrow}, \tag{3.24}$$

$$c^\dagger_{i\uparrow} = \sum_n v^{n}_{i\uparrow}\gamma^{(-E)}_{n\uparrow} + v^{n+N^2}_{i\uparrow}\gamma^{(-E)}_{n\downarrow} + v^{n+2N^2}_{i\uparrow}\gamma^{(E)}_{n\downarrow} + v^{n+3N^2}_{i\uparrow}\gamma^{(E)}_{n\uparrow}, \tag{3.25}$$

$$c^\dagger_{i\downarrow} = \sum_n v^{n}_{i\downarrow}\gamma^{(-E)}_{n\uparrow} + v^{n+N^2}_{i\downarrow}\gamma^{(-E)}_{n\downarrow} + v^{n+2N^2}_{i\downarrow}\gamma^{(E)}_{n\downarrow} + v^{n+3N^2}_{i\downarrow}\gamma^{(E)}_{n\uparrow}. \tag{3.26}$$

But making the following identification:

$$v_{i,\sigma}^{*n} = u_{i,\sigma}^{n+3N^2}, \quad v_{i,\sigma}^{*n+N^2} = u_{i,\sigma}^{n+2N^2}, \\ v_{i,\sigma}^{*n+2N^2} = u_{i,\sigma}^{n+N^2}, \quad v_{i,\sigma}^{*n+3N^2} = u_{i,\sigma}^{n}, \tag{3.27}$$

$$\gamma_{n\sigma}^{\dagger(\pm E)} = \gamma_{n\sigma}^{(\mp E)}, \tag{3.28}$$

the two definitions become the same. This seeming ambiguity stems from the artificial doubling of degrees of freedom one makes when going to the Bogoliubov-de-Gennes formalism. The last four ways of writing the electronic operators are actually writing the corresponding hole operators. Using these to calculate, say, the electron density one would actually count *unoccupied holes* instead of *occupied electrons*. Of course these are completely equivalent statements since the hole and electron spectra are, by construction, mirror images of each other around the chemical potential. Thus we finally find an expression for the energy gap: using (3.17) and (3.24),

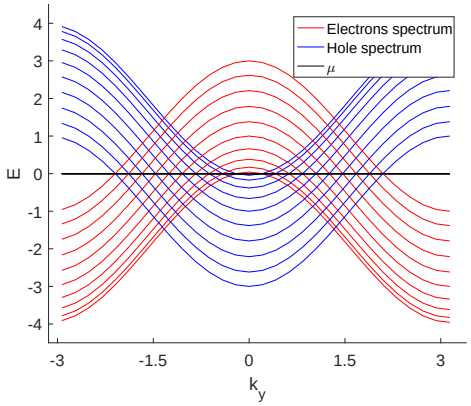

Figure 1: The spectrum of an electron states and their corresponding hole states in the BdG-formalism. For simplicity, only the hopping term is included. μ is fixed at zero energy by construction.

$$\Delta_i = -V_{eff} \sum_n v_{i\downarrow}^{*n} u_{i\uparrow}^{n} f(-E_{n\uparrow}) + v_{i\downarrow}^{*n+N^2} u_{i\uparrow}^{n+N^2} f(-E_{n\downarrow}) \\ + v_{i\downarrow}^{*n+2N^2} u_{i\uparrow}^{n+2N^2} f(E'_{n\downarrow}) + v_{i\downarrow}^{*n+3N^2} u_{i\uparrow}^{n+3N^2} f(E'_{n\uparrow}). \tag{3.29}$$

3.3 Majorana fermions

Majorana fermions are characterized by the property that they are their own antiparticles. This means, that if $\gamma^\dagger$ is the creation operator for a Majorana fermion,

$$\gamma^\dagger = \gamma. \tag{3.30}$$

Looking at (3.28) one sees, that if a quasiparticle state has zero energy the Majorana condition will be fulfilled. Thus, the model described by (3.1) will host Majorana fermions if there exists an eigenstate with zero energy.

4 1D model

In this section we briefly move away from the 2D Hamiltonian in eq. (3.1) to consider a similar 1D model. We wish to classify the system using Table 1 and explore edge states in the topologically non-trivial phases.

4.1 Hamiltonian of 1D topological superconductor

The Hamiltonian under consideration is:

$$H = -t \sum_{\langle i,j\rangle\sigma} c_{i\sigma}^\dagger c_{j\sigma} - \mu \sum_{i\sigma} c_{i\sigma}^\dagger c_{i\sigma} \\ - \gamma B \sum_{i\sigma\sigma'} \sigma_{\sigma,\sigma'}^{(x)} c_{i\sigma}^\dagger c_{i\sigma'} + \sum_i \Delta c_\uparrow^\dagger c_\downarrow^\dagger + h.c \\ + E_{so} \sum_{j\sigma,\sigma'} i \left(c_{j\sigma}^\dagger \sigma_{\sigma,\sigma'}^{(z)} c_{j+\delta_x\sigma'} - h.c. \right). \tag{4.1}$$

It describes the electrons of a 1D crystal with only nearest neighbor hopping, and the electrons are under the influence of the Rashba spin orbit coupling, s-wave superconductivity and a magnetic field in direction of the systems axis which we call the x-axis.

Now a step is taken which is more explicitly explained in the next section, section 5. We assume periodic boundary conditions of the systems edges and Fourier transform the Hamiltonian (4.1). Then, going to the BdG formalism described in section 3, and writing the Hamiltonian with the use of the so called Nambu basis described in section 5, we obtain

$$\begin{aligned}\mathcal{H} = &(-2t\cos(k_x) - \mu)\left[\mathbb{I}^{\sigma}_{2\times 2} \otimes \tau_z\right] - \gamma B\left[\sigma_x \otimes \tau_z\right] \\ &+ 2E_{so}\sin(k_x)\left[\sigma_z \otimes \mathbb{I}^{\tau}_{2\times 2}\right] + \Delta\left[i\sigma_y \otimes i\tau_y\right].\end{aligned} \tag{4.2}$$

How exactly this is done is not essential for this section. For now it is sufficient to know that the symmetries of $\mathcal{H}$ are the symmetries of the Hamiltonian H.
We have assumed periodic boundary conditions, which amounts to considering the bulk of a large system. That is, the study of (4.2) is the study of the bulk eigenenergies of a large but finite 1D system.

The following anti-unitary operators:

$$\mathcal{T} = \sigma_x\tau_z\mathcal{K}, \quad \mathcal{T}^2 = 1 \tag{4.3}$$

$$\mathcal{P} = \tau_x\mathcal{K}, \quad \mathcal{P}^2 = 1, \tag{4.4}$$

have the following commutation relations with the hamiltonian:

$$\mathcal{T}\mathcal{H}(k_x)\mathcal{T}^{-1} = \mathcal{H}(-k_x) \tag{4.5}$$

$$\mathcal{P}\mathcal{H}(k_x)\mathcal{P}^{-1} = -\mathcal{H}(-k_x). \tag{4.6}$$

From these we can construct the operator:

$$\mathcal{C} = \mathcal{T}\mathcal{P} = i\tau_y\sigma_x \tag{4.7}$$

$$\mathcal{C}\mathcal{H}(k_x)\mathcal{C}^{-1} = -\mathcal{H}(k_x), \tag{4.8}$$

which leads us to classify the system as belonging to group BDI in Table 1. As the system is 1 dimensional, this means that there are topologically non-trivial phases of the system.

4.2 Eigenvalues and zero energy conditions

The phase transition from trivial to non-trivial or vice versa occurs under bulk-gap closings[1], that is, when the eigenenergies of (4.2) are 0, as discussed in section 2. Diagonalizing the Hamiltonian, one obtains the following four eigenvalues:

$$E = \pm\sqrt{\gamma^2B^2 + \Delta^2 + L_{so}(k_x)^2 + \epsilon(k_x)^2 \pm 2\sqrt{L_{so}(k_x)^2\epsilon(k_x)^2 + (\epsilon(k_x)^2 + \Delta^2)\gamma^2B^2}}, \tag{4.9}$$

where $\epsilon(k_x) = 2t\cos(k_x) + \mu$ and $L_{so}(k_x) = 2E_{so}\sin(k_x)$. Two of these four eigenvalues can become zero, and only when

$$\gamma^2B^2 + \Delta^2 + L_{so}(k_x)^2 + \epsilon(k_x)^2 - 2\sqrt{L_{so}(k_x)^2\epsilon(k_x)^2 + (\epsilon(k_x)^2 + \Delta^2)\gamma^2B^2} = 0.$$

This condition is fulfilled[1] when,

$$\gamma^2B^2 + L_{so}(k_x)^2 = \Delta^2 + \epsilon(k_x)^2 \tag{4.10}$$

$$L_{so}(k_x)^2\Delta^2 = 0, \tag{4.11}$$

which is only true if $L_{so}(k_x) = 0$, i.e. $k_x = 0$ or $k_x = \pi$, since we assume a constant, non-zero superconducting gap. Inserting $L_{so}(k_x) = 0$ in (4.10), the zero-energy conditions on the parameters are:

$$(2t + \mu)^2 + \Delta^2 = \gamma^2B^2, \quad k_x = 0 \tag{4.12}$$

$$(2t - \mu)^2 + \Delta^2 = \gamma^2B^2, \quad k_x = \pi. \tag{4.13}$$

On Figure 2 is plottet the band structure for the Hamiltonian, with parameters specified in the Figure caption. As is seen, for γB given by (4.12) and (4.13), the bulk gap closes, as expected.

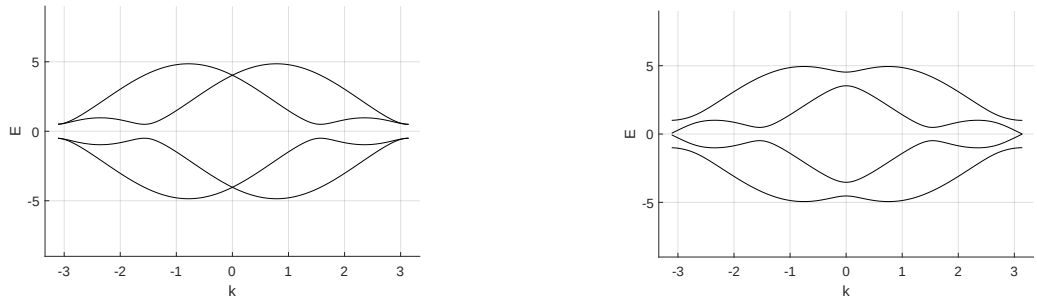

(a) $\gamma B = 0$ (b) $\gamma B = 0.5$

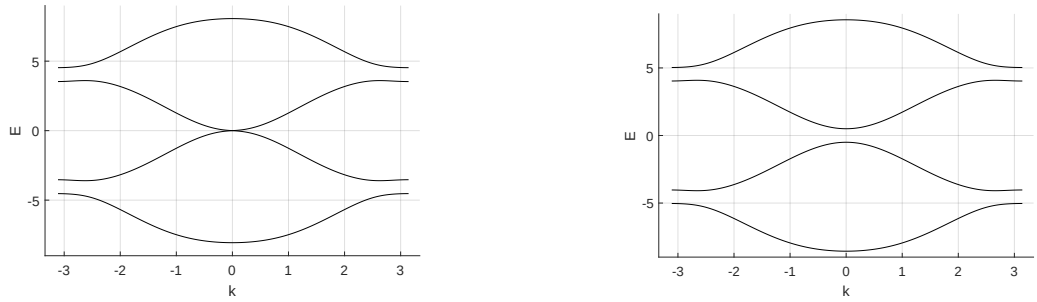

(c) $\gamma B = 4.03$ (d) $\gamma B = 4.53$

Figure 2: Dispersion relation of the nanowire with periodic boundary conditions and 200 crystal sites. Parameter values: $\mu = 2$, $t = 1$, $E_{so} = 1$ and $\Delta = 0.5$.

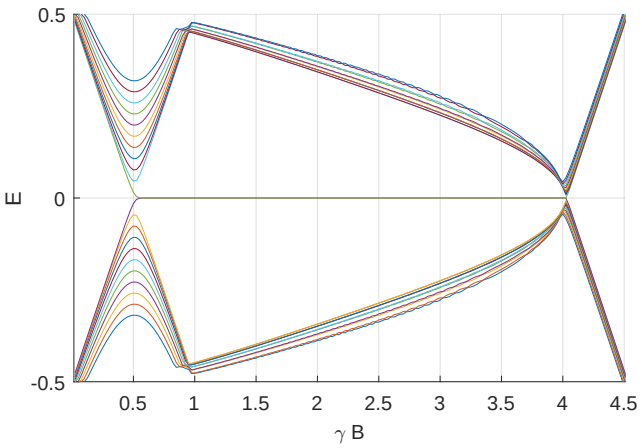

Figure 3: A few chosen eigenenergies as a function of γB of the nanowire with open boundary conditions and 200 crystal sites. All parameters other than γB are chosen as in Fig. 2 . As can be seen, in the interval between two bulk gap closings there are two stable zero-energy states.

4.3 Protected zero energy edge states

Going back to the real-space version of (4.2), we can impose open boundaries and numerically calculate the eigenvalues similarly to how it was described in section 3. On Fig. 3 is plotted the smallest eigenvalues of such a system as a function of the external B field. As can be seen, 0 energy states appear around the value of $\gamma B = 0.5$ that corresponds to a bulk gap closing in Fig. 2b, and they dont dissappear until the bulk gap closes again at $\gamma B = 4.03$. On Fig. 4 the two zero energy states and one state with non-zero energy are shown. As can be seen, the two zero energy states are confined to the edges of the wire,

while the non-zero energy state is not. This is only the case when γB is at a value between the two bulk gap closings. Outside this region, there are no zero-energy states and in general no edge states. This regime is the topologically non-trivial phase of the 1D system, and the correspondence between the bulk gap closings and the appearence of zero energy edge states is called the bulk-boundary correspondence. Lastly we mention that since the energies of the states are 0, and these states are the quasiparticle states defined in the same way as in section 3, the states are Majorana fermions.

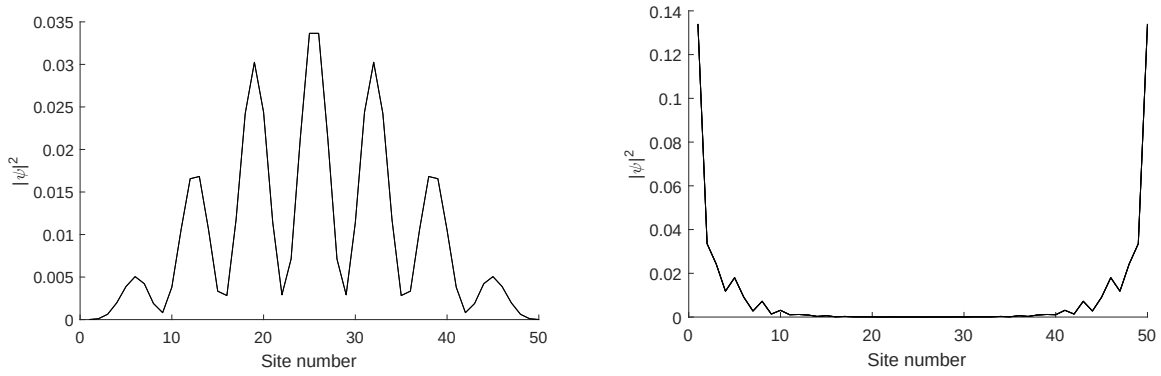

(a) A non-zero energy state

(b) The two zero energy states

Figure 4: The zero-energy states and a non-zero energy state plotted in real space. As is clear, the zero-energy states are confined to the edges of the sample. We have here used a crystal with 50 sites for a clearer picture of the edge states. The parameters all have the same value as in Fig. (2) and $\gamma B = 1.5$

.

5 2D model

We now turn back to the 2D model. There will not be any calculations regarding the Chern number of the system. Instead the focus is on numerical calculations and it is through these that we study the different phases of the system.
Generally, the calculations made are not self-consistent, i.e. we have not demanded (3.29) be true, since it does not make a difference in characterizing the phases. Two exceptions are made, in order to calculate the temperature dependency of the superconducting gap.

5.1 The Hamiltonian and its symmetries

Imposing periodic boundary conditions on the Hamiltonian in (3.1) and Fourier transforming it, we obtain:

$$H = -\sum_{\mathbf{k},\sigma,\sigma'} \left(\epsilon(\mathbf{k}) \mathbb{I}_{\sigma,\sigma'} + \gamma B \sigma^{(z)}_{\sigma,\sigma'} - \mathbf{E}_{so}(\mathbf{k}) \cdot \boldsymbol{\sigma}_{\sigma,\sigma'} \right) c^\dagger_{\mathbf{k}\sigma} c_{\mathbf{k}\sigma'} + \sum_{\mathbf{k}} \Delta(\mathbf{k}) c^\dagger_{\mathbf{k}\uparrow} c^\dagger_{-\mathbf{k}\downarrow} + \Delta^*(\mathbf{k}) c_{-\mathbf{k}\downarrow} c_{\mathbf{k}\uparrow}, \quad (5.1)$$

Here $\epsilon(\mathbf{k}) = -\left(2t(\cos(k_x) + \cos(k_y)) + \mu\right)$ and $\mathbf{E}_{so} = E_{so}\left(\sin(k_y), -\sin(k_x), 0\right)$. The superconducting energy gap is given by

$$\Delta(\mathbf{k}) = -V_{eff} \sum_{\mathbf{k}} \langle c_{-\mathbf{k}\downarrow} c_{\mathbf{k}\uparrow} \rangle \,, \qquad \Delta^*(\mathbf{k}) = -V_{eff} \sum_{\mathbf{k}} \langle c^\dagger_{\mathbf{k}\uparrow} c^\dagger_{-\mathbf{k}\downarrow} \rangle \,. \quad (5.2)$$

To diagonalize the Hamiltonian we use the BdG formalism as in section 3, using the anti-commutation relations of fermions. Written in the so called Nambu basis:

$$\begin{pmatrix} c^\dagger_{\mathbf{k}\uparrow} & c^\dagger_{\mathbf{k}\downarrow} & c_{-\mathbf{k}\uparrow} & c_{-\mathbf{k}\downarrow} \end{pmatrix} = \begin{pmatrix} \mathbf{c}^\dagger_{\mathbf{k}} & \mathbf{c}_{-\mathbf{k}} \end{pmatrix}$$

$$\begin{pmatrix} c_{\mathbf{k}\uparrow} \\ c_{\mathbf{k}\downarrow} \\ c^\dagger_{-\mathbf{k}\uparrow} \\ c^\dagger_{-\mathbf{k}\downarrow} \end{pmatrix} = \begin{pmatrix} \mathbf{c}_{\mathbf{k}} \\ \mathbf{c}^\dagger_{-\mathbf{k}} \end{pmatrix}$$

we can write the Hamiltonian as a matrix product:

$$H = \begin{pmatrix} \mathbf{c}^\dagger_{\mathbf{k}} & \mathbf{c}_{-\mathbf{k}} \end{pmatrix} \begin{pmatrix} \widehat{H_0}(\mathbf{k}) & i\sigma_y\Delta \\ -i\sigma_y\Delta^* & -\widehat{H_0}^T(-\mathbf{k}) \end{pmatrix} \begin{pmatrix} \mathbf{c}_{\mathbf{k}} \\ \mathbf{c}^\dagger_{-\mathbf{k}} \end{pmatrix} = \begin{pmatrix} \mathbf{c}^\dagger_{\mathbf{k}} & \mathbf{c}_{-\mathbf{k}} \end{pmatrix} \mathcal{H} \begin{pmatrix} \mathbf{c}_{\mathbf{k}} \\ \mathbf{c}^\dagger_{-\mathbf{k}} \end{pmatrix}. \tag{5.3}$$

Where we have used, that

$$\Delta(\mathbf{k}) = \Delta(-\mathbf{k}), \qquad \Delta^*(\mathbf{k}) = \Delta^*(-\mathbf{k}), \tag{5.4}$$

This is due to the electrons forming the Cooper pairs being in the spin singlet state in this model, since we consider s-wave superconductivity. From the definition of the superconducting energy gap (5.2), the gap must be even under exchange of $\mathbf{k}$-vectors of the electrons, since it is odd under exchange of spin and must be and odd function of overall exchange between electrons. We refer to appendix I for an explicit calculation of $\mathcal{H}$.

The 1st and 4th quadrants in $\mathcal{H}$ couple creation-annihilation operators of the same wave-vector, but possibly differing spins, while the 2nd and 3rd couple operators of opposite wave-vectors. In the same way the Pauli-matrices can be used to couple opposite spins, we can use pseudo Pauli-matrices to couple opposite wave-vectors. We will denote the pseudo Pauli-matrices $\boldsymbol{\tau}$, and then work in two spaces, one in the basis of spins and one in the basis of wave-vectors. Then we can write (5.3) as

$$\begin{aligned} \mathcal{H} = &(-2t(\cos(k_x) + \cos(k_y) - \mu)\left[\mathbb{I}^\sigma_{2\times 2} \otimes \tau_z\right] - \gamma B\left[\sigma_z \otimes \tau_z\right] \\ &+ E_{so}\left(\sin(k_y)\left[\sigma_x \otimes \mathbb{I}^\tau_{2\times 2}\right] - \sin(k_x)\left[\sigma_y \otimes \tau_z\right]\right) + \Re(\Delta)\left[i\sigma_y \otimes i\tau_y\right] + \Im(\Delta)\left[-\sigma_y \otimes \tau_x\right]. \end{aligned} \tag{5.5}$$

Using this form, we can find symmetry operators of the Hamiltonian to classify the system in Table 1. First we observe that time-reversal symmetry is broken by the external magnetic field leading to the Zeeman term in the Hamiltonian. But since the BdG Hamiltonian is by construction anti-symmetric in electrons and holes, it should exhibit charge conjugation symmetry

$$\mathcal{P}^\dagger\mathcal{H}(\mathbf{k})\mathcal{P} = -\mathcal{H}(-\mathbf{k}), \tag{5.6}$$

and a system exhibiting charge-conjugation symmetry and no time-reversal symmetry cannot exhibit chiral symmetry, as discussed in section 2. If we can find an operator $\mathcal{P}$, the system belongs to the symmetry class D or C, and has a topologically non-trivial phase. Consider the operator

$$\mathcal{P} = \tau_x\mathcal{K}, \tag{5.7}$$

which is an anti-unitary operator. Using this operator, and observing that

$$\sigma_a\sigma_b\sigma_a = \begin{cases} +\sigma_b & \text{if } b = a \\ -\sigma_b & \text{if } b \neq a \end{cases}, \tag{5.8}$$

we find the condition (5.6) fulfilled. Note that the operators $\sigma_{x,y,z}$ commute with the operators $\tau_{x,y,z}$, since they are operators on different spaces. Finally observe that

$$\mathcal{P}^2 = 1, \tag{5.9}$$

which leads us to conclude that the system belongs to the symmetry class D.

5.2 Eigenvalues and zero-energy condition

The superconducting gap Δ generally depends on $\mathbf{k}$, but we will, from now on and until otherwise stated, treat it as a constant. The eigenvalues of the Hamiltonian, $\mathcal{H}$, in eq. (5.3) can now be found

$$E(\mathbf{k}) = \pm\sqrt{\epsilon(\mathbf{k})^2 + |\Delta|^2 + \gamma^2B^2 + \mathbf{E_{so}}(\mathbf{k})^2 \pm 2\sqrt{\epsilon(\mathbf{k})^2\mathbf{E_{so}}(\mathbf{k})^2 + \left(\epsilon(\mathbf{k})^2 + |\Delta|^2\right)\gamma^2B^2}}. \tag{5.10}$$

As in section 4, we follow [1] to determine conditions for zero energy eigenvalues. First of all, we can only obtain 0 energy eigenvalues if:

$$\epsilon(\mathbf{k})^2 + |\Delta|^2 + \gamma^2 B^2 + \mathbf{E_{so}}(\mathbf{k})^2 - 2\sqrt{\epsilon(\mathbf{k})^2 \mathbf{E_{so}}(\mathbf{k})^2 + \left(\epsilon(\mathbf{k})^2 + |\Delta|^2\right)\gamma^2 B^2} = 0. \tag{5.11}$$

A solution is obtained if:

$$\epsilon(\mathbf{k})^2 + |\Delta|^2 = \gamma^2 B^2 + \mathbf{E_{so}}(\mathbf{k})^2, \tag{5.12}$$

$$|\Delta|^2 \mathbf{E_{so}}(\mathbf{k})^2 = 0 \tag{5.13}$$

The superconducting gap energy is assumed constant and non-zero, which means that (5.13) is only fulfilled for $\mathbf{E_{so}}(\mathbf{k}) = 0$, which means the wavefunction with zero energy necessarily has wavevector $\mathbf{k} = (0,0), (0,\pi), (\pi,0), (\pi,\pi)$. Using these restricted wavevectors in eq. (5.12) we obtain:

$$(4t+\mu)^2 + |\Delta|^2 = \gamma^2 B^2, \quad \mathbf{k} = (0,0), \tag{5.14}$$

$$\mu^2 + |\Delta|^2 = \gamma^2 B^2, \quad \mathbf{k} = (0,\pi), (\pi,0), \tag{5.15}$$

$$(4t-\mu)^2 + |\Delta|^2 = \gamma^2 B^2, \quad \mathbf{k} = (\pi,\pi), \tag{5.16}$$

which are the conditions for closing the bulk gap of the 2D system.

5.3 Semi-periodic boundary condition

In this subsection we choose Δ to be real, as only its absolute value has an effect on the topology of the system. We impose open boundary conditions in the x-direction of the crystal but keep periodic boundary conditions in the y-direction of the crystal. The periodic boundary conditions enable us to write (3.1) in the (x, k_y)-basis by Fourier transform in the y-direction. In this basis, the Hamiltonian is:

$$\begin{aligned} H = &-t \sum_{i_x,\delta_x,k_y,\sigma,\sigma'} \mathbb{I}^{2\times 2}_{\sigma,\sigma'} \left(2\cos(k_y) c^\dagger_{i_x,k_y,\sigma} c_{i_x,k_y,\sigma'} + (c^\dagger_{i_x+\delta_x,k_y,\sigma} + c^\dagger_{i_x-\delta_x,k_y,\sigma}) c_{i_x,k_y,\sigma'}\right) \\ &- \mu \sum_{i_x,k_y,\sigma,\sigma'} \mathbb{I}^{2\times 2}_{\sigma,\sigma'} c^\dagger_{i_x,k_y,\sigma} c_{i_x,k_y,\sigma'} \\ &+ E_{so} \sum_{i_x,k_y,\sigma,\sigma',\delta_x} -2\sin(k_y) c^\dagger_{i_x,k_y,\sigma} \sigma^{(x)}_{\sigma,\sigma'} c_{i_x,k_y,\sigma'} + i\sigma^{(y)}_{\sigma,\sigma'} \left(c^\dagger_{i_x,k_y,\sigma} c_{i_x+\delta_x,k_y,\sigma'} - h.c.\right) \\ &- \gamma B \sum_{i_x,k_y,\sigma,\sigma'} c^\dagger_{i_x,k_y,\sigma} \sigma^{(z)}_{\sigma,\sigma'} c_{i_x,k_y,\sigma'} + \sum_{i_x,k_y} \Delta c^\dagger_{i_x,k_y,\uparrow} c^\dagger_{i_x,-k_y,\downarrow} + h.c. \end{aligned} \tag{5.17}$$

Due to the open boundary conditions, we cannot write the Hamiltonian purely in the k-basis. Thus the previous analytical method of finding eigenvalues of H cannot be applied. Instead we numerically diagonalize (5.17) to find eigenenergies.

Since there are three bulk-gap closings, there are four regimes of the system, and the topological phase of each of these four regimes depends on where the value of μ falls [1] in the ranges:

$$\mu \leq -2t, \quad -2t < \mu \leq 0 \quad 0 < \mu \leq 2t, \quad 2t < \mu. \tag{5.18}$$

On Figure 5 is shown the dispersion relation, $E(k_y)$ of all states in a crystal of 30-by-30 sites. The parameters used are specified in the caption.

As can be seen, there are states with zero-energy for $\gamma B = 2$ and $\gamma B = 3$. Further, from Fig. 6a one sees that for γB between approximately 1.75 and 6.75, states exist with energy around 0. This fits with the gap closing conditions (5.14) and (5.16) as, with the parameters written Figure 5,

$$(4t+\mu)^2 + |\Delta|^2 = 1.80 \tag{5.19}$$

$$(4t-\mu)^2 + |\Delta|^2 = 6.58. \tag{5.20}$$

Apparently, between two bulk gap-closings there exist protected zero-energy states. This is just as was shown in the 1D crystal. But contrary to the 1D system, in 2D there exists a third bulk gap-closing

condition, the crossing of which does not remove zero-energy states. This was for $\mu < -2t$. For plots similar to Fig. 6 with μ in the other ranges in (5.18) see appendix E. There we see that no matter where μ falls there are two non-trivial topological regimes of the system, and two trivial.
Looking closely at the energies nearest 0 in Fig. 6a one observes that they oscillate. In Fig. 6b a system with 50-by-50 sites has been chosen and the oscillations have disappeared. This was checked for smaller and bigger sized systems, and for smaller systems the oscillations were more pronounced while for bigger systems they disappeared. An interpretation of this is that the two edge states, when in a smaller system, are able to affect each other, which results in the oscillations [2]. Thus to create true edge states one needs a large enough system, that the two states die before reaching each other.

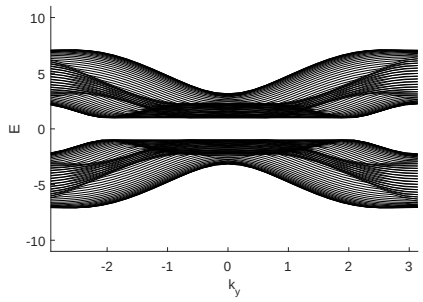

(a) $\gamma B = 0$

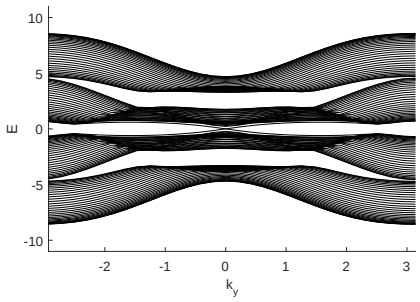

(b) $\gamma B = 2$

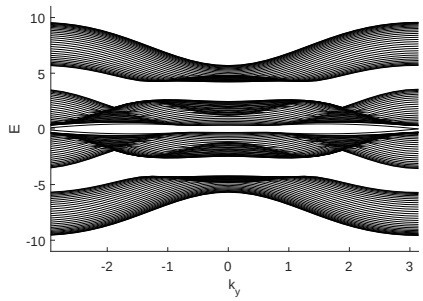

(c) $\gamma B = 3$

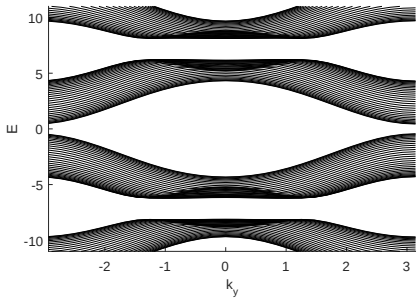

(d) $\gamma B = 7$

Figure 5: Dispersion relation of the 2D crystal with 30 crystal sites in the x-direction. Parameter values: $\mu = -2.5$, $t = 1$, $E_{so} = 0.75$ and $\Delta = 1$.

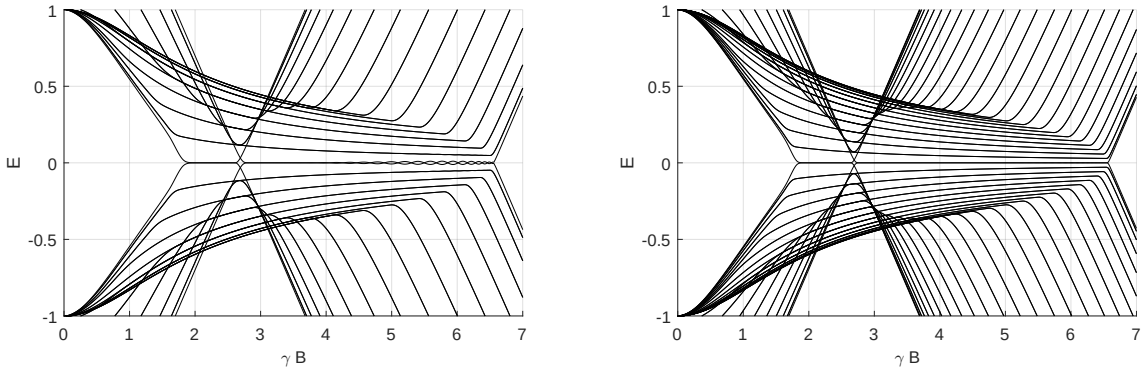

(a) (b)

Figure 6: Energy as a function of external B-field for a few chosen low energi eigenstates in the 30-by-30 crystal. In (b) is shown the same plot for a system of 50-by-50 sites. As is seen, the oscillatory behavior of the energy near $E = 0$ is gone.

5.4 Chiral edge-states

On Fig. 7a and 7b is shown one of the lowest energy eigenstates for positive and negative k_y. As is seen, the sign of the momentum chooses one edge of the crystal to confine the state to. Using Fig. 5b to find the slope of the spectrum for these states it is possible to determine the sign of the group velocity. Looking, for example, at the smallest negative energy state, the slope changes sign at $k_y = 0$. Thus, on opposite sides of the system the states move in opposite directions. States behaving like this are called chiral edge-states.

The zero-energy edge states have also been calculated, and were found to be localized on both edges of the system. A plot of one of these states is shown in appendix F. Since they have zero energy, they are Majorana fermions. Thus the Majorana fermions in this system are also confined to the edges, similarly to the 1D system. When moving out of the regime with zero-energy states in Fig. 6 it was found that no states were confined to an edge.

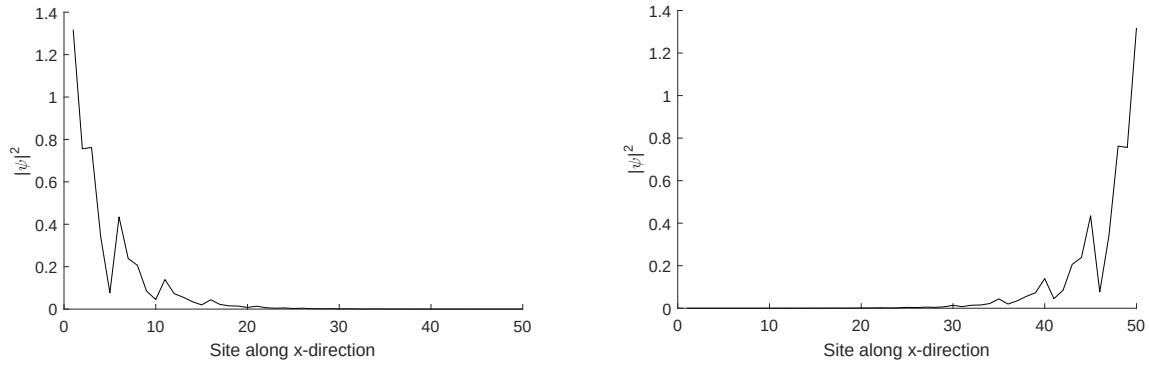

(a) $k_y = -0.13$ (b) $k_y = 0.13$

Figure 7: The wavefunction for lowest-energy states with opposite momentum. The two states are confined each at their own edge. This indicates that the their dispersion is chiral. 50 sites along the x-direction has here been chosen instead of 30 to better illustrate the confinement. Here $\gamma B = 2$.

5.5 Local density of states

One of the experimentially observable quantities is the local density of states (LDOS), and is therefore interesting to calculate numerically. on Fig. 8 is seen the LDOS at the edge and in the bulk of system. These signatures can be used to find whether Majorana states are present in an experimental sample. As can be seen, the most significant difference between the edge and the bulk of the system is the appearance of zero energy states at the edge. The energy axes have purposefully been limited to be near 0, since the important difference between the LDOS at the edge and the bulk of the system is at $E = 0$. For a comparison with the corresponding LDOS in the trivial regime see appendix G. This reveals that one can use the appearence of a finite density at $E = 0$ as an indicator of being in a non-trivial phase.

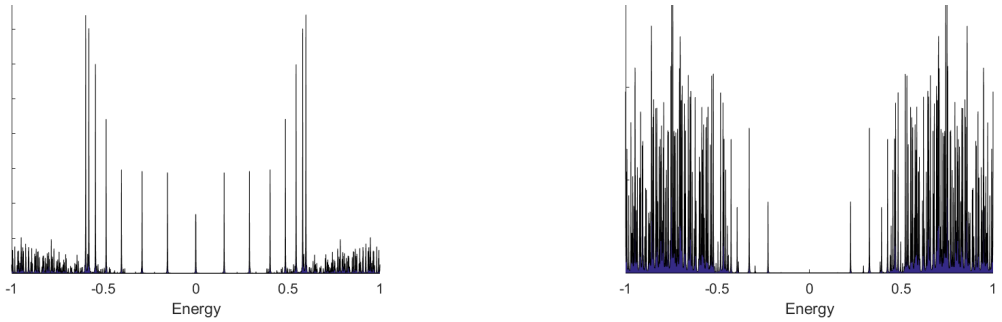

(a) Site number 1 in the x-direction (edge site)

(b) Site number 15 in the x-direction (bulk site)

Figure 8: LDOS at an edge site and at a bulk site.

5.6 Suppression of the critical temperature in the topological phase

In this subsection the temperature dependency of the superconducting gap is found in topologically trivial and non-trivial phases of the semi-periodic system. The numerical calculations must therefore be done self-consistently. In Fig. 9 the plot showing the result of this calculation is shown. What it shows is that the critical temperature, the temperature where the superconducting gap becomes zero, is supressed in the topologically non-trivial phase. This may serve as another indicator of being in a non-trivial regime.

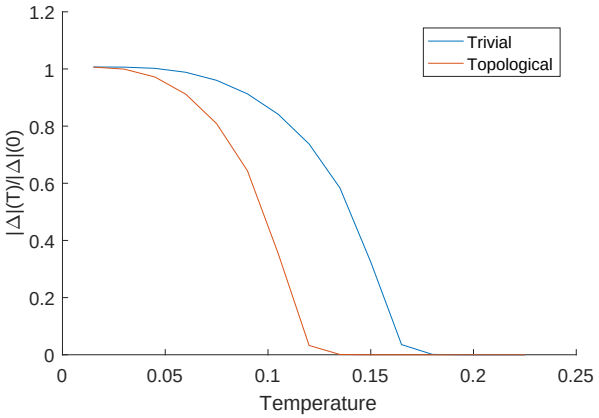

Figure 9: The superconducting gap as a function of temperature in both the trivial and non-trivial phases of the system. Here $|\Delta| = 0.35$ and $\gamma B = 2$ in the topological phase and $\gamma B = 1$ in the trivial phase. The rest of the parameters are chosen as in Fig. 5

5.7 Vortex induced Majorana states

With the method of numerically diagonalizing the real space Hamiltonian (3.1) adding real space dependencies of the parameters in the model is possible. Here we will add a space-dependent phase to the superconducting gap and explore the effect on the states of the system.
Starting from a 25-by-25 site system and imposing open boundaries at all edges, we introduce a vortex-behaving phase to the superconducting gap,

$$\Delta \to \Delta e^{im\theta} \tag{5.21}$$

placing the vortex-core in the middle of the system. The winding number of the phase m is set to 1 in the following.
One requirement for being in a topologically non-trivial regime is [1][2],

$$\sqrt{(4t-\mu)^2+|\Delta|^2} < \gamma B < \sqrt{\mu^2+|\Delta|^2} \tag{5.22}$$

for $\mu > 2t$. We choose the parameters $t = 1$ and $\mu = 4$ for the system, simplifying (5.22) to

$$|\Delta| < \gamma B < \sqrt{\mu^2+|\Delta|^2}, \tag{5.23}$$

which here becomes the requirement for the bulk system to be in the non-trivial phase. Adding a vortex to the system with Chern number p and winding number of the vortex m, the topological invariant, ν, of the system becomes a type $\mathbb{Z}_2$ invariant where[5],

$$\nu = pm \mod 2. \tag{5.24}$$

Since we have chosen a winding number $m = 1$, $\nu \neq 0$ if the Chern number is odd. It is possible, therefore, that therefore the system is in a non-trivial topological phase if (5.23) is fulfilled.

Due to the mixing of the lowest energy state for small systems, discussed in the context of the semi-periodic system, $E \approx 0$ for these states but are not exactly zero even in the topological regime. Limitations of the computer RAM prevents going to large enough systems that this is not an issue. A sweep over γB has been made, like in Fig. 6, and a specific value for γB has been chosen such that, at that exact value, the lowest energy states are zero-energy states.
Plotting the lowest energy eigenstates both outside and inside the non-trivial regimes, the lowest energy eigenstates are confined around the vortex. To distinguish the Majorana states from other low energy states, a basis change is performed [2],

$$\gamma_1 = \frac{1}{\sqrt{2}}\left(\gamma_+ + \gamma_-\right),$$
$$\gamma_2 = \frac{1}{\sqrt{2}}\left(\gamma_+ - \gamma_-\right),$$

where γ_+ and γ_- are the old lowest energy states. This should be possible in the topologically non-trivial regime, as the two states have approximately zero energy (and have exactly zero energy for large systems), and thus belong to the same degenerate subspace. Plots of these new states is shown in Fig. 10. As is observed, these states split into one confined to the edge of the system and one confined to the area around the vortex. Only for the Majorana states is this type of splitting observed, which enables distinguishing Majorana states from the other low energy states.

The LDOS of four chosen sites are shown in Fig. 11. The energy axis has been zoomed in so as to better see the LDOS near $E = 0$. These indicate that the zero-energy states are confined to near the core and the edge of the system. In appendix H is shown the LDOS for a value of γB which is in the trivial regime. Like in the case of the semi-periodic system, the appearance of finite density at $E = 0$ distinguishes the non-trivial from the trivial phase.

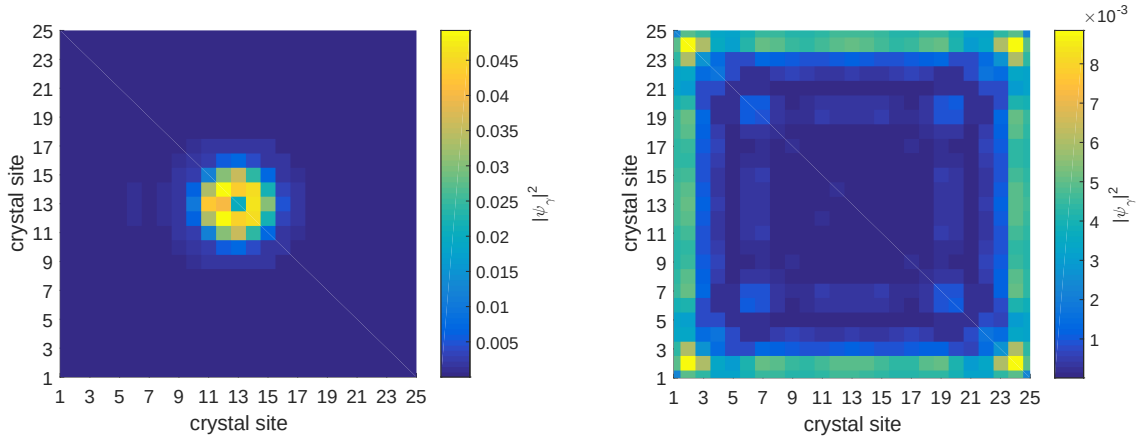

(a) Majorana at vortex edge.

(b) Majorana at crystal edge

Figure 10: The two Majorana fermions in a finite, 25-by-25 sites system with a vortex in the phase of the superconducting gap. Parameters: $t = 1$, $\mu = 4$, $E_{so} = 0.56$, $t = 1$, $\gamma B = 0.903$.

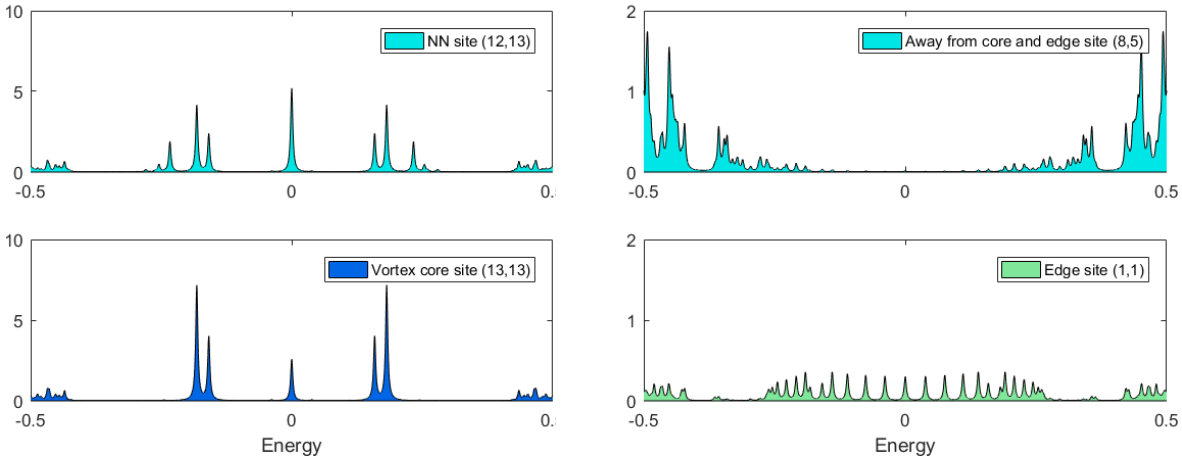

(a)

(b)

Figure 11: (a) LDOS at the vortex core and a nearest neighbor site. (b) LDOS at a site away from the core and the edge of the crystal and at an edge site.

5.8 On-site-potential impurities

In this subsection we study a system with periodic boundary conditions but with one impurity implemented as an on-site-potential. The purpose is to see whether zero-energy states appear near the edge defined by the impurity, if the system is in the non-trivial phase

We choose a 15-by-15 sites crystal, impose periodic boundary conditions and introduce a term

$$-V_{imp} \sum_{\sigma} c^{\dagger}_{(8,8)\sigma} c_{(8,8)\sigma}, \tag{5.25}$$

i.e. a potential on the site (8,8) in the Hamiltonian (3.1). Here V_{imp} defines the impurity strength. Originally the calculations were meant to be done self-consistently. This was due to the supression of $|\Delta|$ on a site of a strong impurity. But on the site of a strong impurity, the actual value of $|\Delta|$ will not considerably change the LDOS on the impurity site, since this will be dominated by the impurity strength. Thus we chose to do a non-self-consistent calculation in this section as well.
In Fig. 12 (Fig. 13) are shown the LDOS at two different sites, one near the impurity, the other far from the impurity in the bulk systems non-trivial (trivial) topological phases. Fig. 12 show that after

some initial change to the LDOS due to the impurity, no increase in its strength creates zero-energy states near the impurity, contrary to the case of a vortex core in the crystal. Comparing Fig. 12 and 13 there is no qualitative difference in the LDOS between the non-trivial and trivial topological phases, and these kind of impurities can therefore not be used to distinguish the non-trivial and trivial phases of the system. Sweeping γB through a range from 0 to 7 showed that indeed a kind of oscillating behavior similar to that in the case of the vortex appeared, but contrary to the vortex, for no value of γB did the smallest energies actually become zero. The conclusion here is that it seems the single site impurity cannot induce zero energy states, but since we are limited in increasing the systems size, it cannot be certainly concluded, and it would therefore be interesting to see if one could determine this analytically.

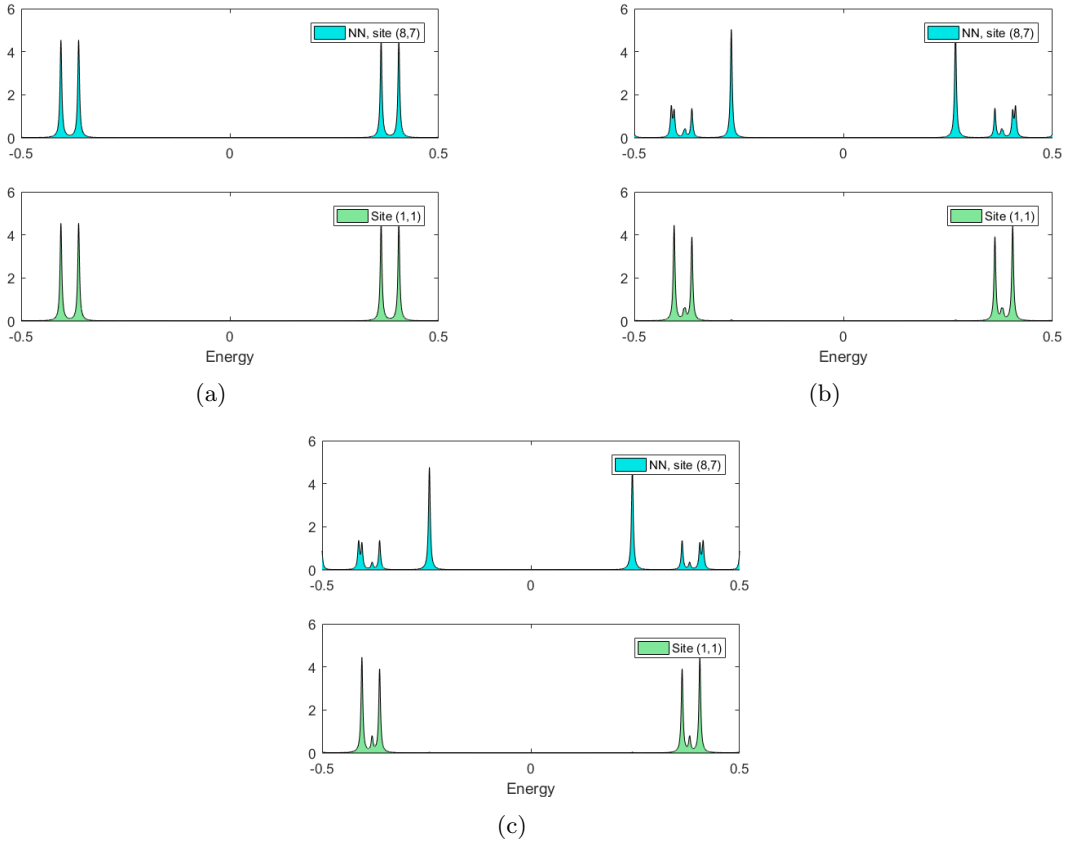

Figure 12: In the non-trivial phase; LDOS at a nearest neighbor to the impurity and far from the impurity with (a) $V_{imp} = 0$, (b) $V_{imp} = 10$ and (c) $V_{imp} = 50$. Here $t = 1$, $\mu = 4$, $E_{so} = 0.5$, $|\Delta| = 0.5$ and $\gamma B = 1$.

A similar calculation was made in the 1D system. In this case, zero-energy states did appear in the non-trivial phases if the impurities were strong enough. This indicates a rather obvious difference in how a single-site impurity acts between the 1D and 2D systems. In the 1D system, a strong impurity separates completely the two pieces on either side of the impurity. The impurity acts as an edge in the 1D system, while this is not the case in 2D.
Another, self-consistent, calculation was done for a 11-by-11 system with an impurity in the middle. The smaller system is chosen due to the greater demands on computational power when implementing self-consistency. In Fig. 14 the temperature dependency of the gap in this system is shown. Similarly to what was the case in the semi-periodic system, the critical temperature is suppressed in the topologically non-trivial phase. In contrast to the semi-periodic system though, it is not a big suppression. Looking at Fig. 12 and Fig. 13, there is a finite density at lower energies in the non-trivial vs. the trivial phase. This suggests that the appearance of small energy states (ideally zero energy states) suppress the critical temperature.

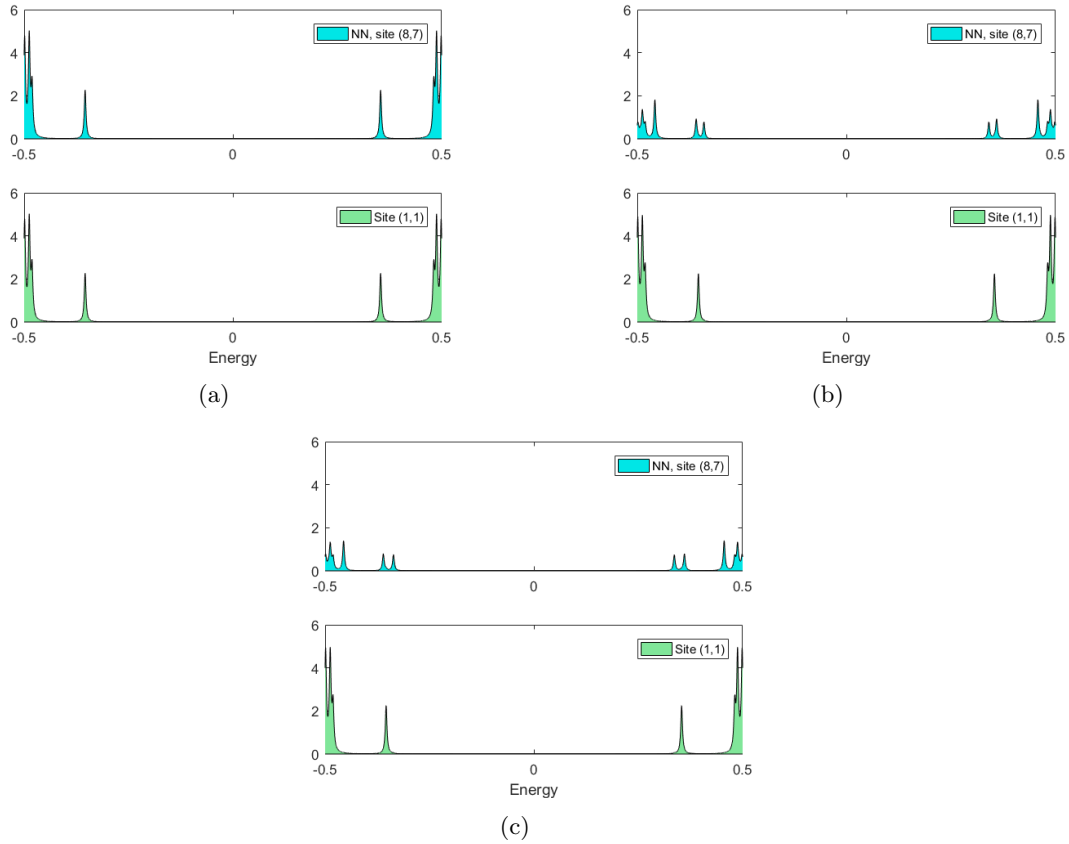

Figure 13: In the trivial phase; LDOS at a nearest neighbor to the impurity and far from the impurity with (a) $V_{imp} = 0$, (b) $V_{imp} = 10$ and (c) $V_{imp} = 50$. Here $t = 1$, $\mu = 4$, $E_{so} = 0.5$, $|\Delta| = 0.5$ and $\gamma B = 0.3$.

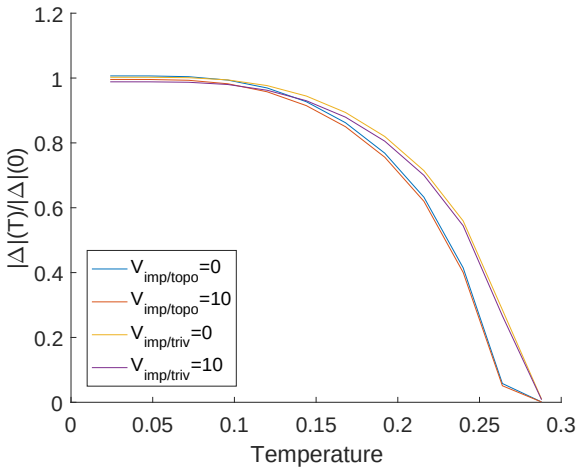

Figure 14: The superconducting gap as a function of temperature in both the trivial and non-trivial phases of the system. Here $|\Delta| = 0.5$ and $\gamma B = 0.3$ in the topological phase and $\gamma B = 0.1$ in the trivial phase. The rest of the parameters are chosen as in Fig. 12

6 Conclusion

In this thesis the topological phases of a 2D crystal consisting of a square lattice affected by s-wave superconductivity, Rashba spin-orbit coupling and a perpendicular, external magnetic field have been explored. The Hamiltonian has been diagonalized using the Bogoliubov-de-Gennes formalism, and the eigenstates, quasiparticle states that are superpositions of electron/hole states, have been described. It has been shown that if such a system has open boundaries in one direction, chiral edge states with two zero-energy states appear in certain parameter regimes. Due to these states having zero energy, the quasiparticles associated with the states have been identified with Majorana fermions.

Inserting a vortex-like phase with winding number $m = 1$ in a system with completely open boundaries it has been shown that zero-energy states appear, and that one is confined near the core of the vortex and the other near the edges of the lattice. An issue regarding oscillating behavior of the smallest-energy states has been found and it has been connected with the finite size of the lattice, which mixes the two states. Due to computational limitations, a larger system could not be used for the case of completely open boundaries, but similar behavior was identified in the system of semi-open boundaries and here the oscillations disappeared for larger systems.

Finally, we explored whether an on-site-potential impurity would induce zero-energy states similarly to what a vortex does. It was found that in 2D this was not the case. A similar test was done in 1D, and here the impurity, if strong enough, did induce zero-energy states. This was interpreted as due to the fact that an on-site-potential in 1D, if strong enough, serves as a true edge of the system, while this is not the case in 2D.

Future work in this specific area could include calculating the Chern number and establish analytical arguments for or against the numerical results in this thesis. One could also introduce magnetic impurities to the system and explore if these could induce zero-energy states. Some of the numerical methods used are quite general, so other topological systems, perhaps a topological insulator, could also be explored numerically.

References

[1] Masatoshi Sato, Yoshiro Takahashi and Satoshi Fujimoto, *Non-Abelian topological orders and Majorana fermions in spin-singlet superconductors*, Physical Review B 82, 134521, (2010).

[2] Kristofer Björnson, *Topological band theory and Majorana fermions*. Retrieved from Digital Comprehensive Summaries of Uppsala Dissertation from the Faculty of Science and Technology (2016).

[3] James F. Annett, (2004) *Superconductivity, Superfluids and Condensates*, New York: Oxford University Press.

[4] Henrik Bruus and Karsten Flensberg (2004) *Many-Body Quantum Theory in Condensed Matter Physics*, New York: Oxford University Press.

[5] Jeffrey C. Y. Teo and C. L. Kane, *Topological defects and gapless modes in insulators and superconductors*, Physical Review B 82, 115120, (2010).

[6] Andrei Bernevig with Taylor L. Hughes (2013), *Topological insulators and topological superconductors.*, New Jersey: Princeton University Press.

[7] M. Z. Hasan and C. L. Kane, *Colloquium: Topological insulators*, Reviews of Modern Physics, Vol. 82, 3045, (2010).

Appendices

A Second quantization formalism

In this appendix the second quantization formalism of quantum mechanics is introduced. The focus will be on fermions, as these are of primary interest in this thesis. This formalism provides a simpler and more intuitive way of describing the systems in the rest of the thesis.

Bosons and fermions

A system of N particles can be described with a state function in real space,

$$\Psi(\mathbf{r}_1, \mathbf{r}_2, ..., \mathbf{r}_N), \tag{A.1}$$

where the $\mathbf{r}_n$'th argument of the function refer to the n'th particle. When describing a system of indistinguishable particles a certain problem shows up: what happens to the state function when two particles are interchanged. Since the particles are indistinguishable, upon interchange of two particles, the new state function must be at least proportional to the old one, and for the state function to be unambiguous we must demand that twice interchanging the particles leaves the state function invariant. Thus, if C is an operator interchanging two particles in the state function we must demand:

$$C^2(\psi(\mathbf{r}_1, \mathbf{r}_2, ..., \mathbf{r}_N)) = \lambda^2\psi(\mathbf{r}_1, \mathbf{r}_2, ..., \mathbf{r}_N) = \psi(\mathbf{r}_1, \mathbf{r}_2, ..., \mathbf{r}_N), \tag{A.2}$$

leaving two options for the action of the C-operator on the state function, namely adding a prefactor $\lambda = \pm 1$. When two particles in the system are interchanged but this leaves the state function invariant the particles are called bosons. If the state function changes sign they are called fermions.
It is possible to show that the state function (A.1) can be written as a product of single particle states:

$$\psi(\mathbf{r}_1, \mathbf{r}_2, ..., \mathbf{r}_N) = \sum_{\nu_1,...,\nu_N} A_{\nu_1,...,\nu_N}\psi_{\nu_1}(\mathbf{r}_1)\cdots\psi_{\nu_N}(\mathbf{r}_N), \tag{A.3}$$

where the sum over index ν_n is a sum over a complete and orthonormal single particle basis and $A_{\nu_1,...,\nu_N}$ refers to a complex number. This construction is valid as a state, but is generally neither symmetric or antisymmetric under particle exchange. Therefore, in the case of a fermionic system, one uses a Slater determinant, and the state function becomes antisymmetric by contruction. Similarly one uses a so called permanent (sign less determinant) for generating a bosonic state function.

Creation and annihilation operators

The vacuum state $|0\rangle$ is defined as an empty state in which one can "fill" particles into different one particle states. The operators filling the state are called creation operators and those emptying it are called annihilation operators. In the case that one creates/annihilates fermions, these operators are denoted $c^\dagger$ and c respectively.
Now, given a set of creation operators $c^\dagger_{\nu_j}$, where ν_j denotes the single particle state filled, one can act with these on the vacuum state to fill it up, so to speak, thereby creating a state (A.3). The corresponding annihilation operators are c_{ν_j}. If one tries to act with c_{ν_j} on a state empty in ν_j, the result is by definition 0. Further, due to the Pauli exclusion principle, only one fermion can occupy a one-particle state in the system. Thus

$$(c^\dagger_{\nu_j})^2\,|0\rangle = 0 \;\; (c_{\nu_j})^2\,|0\rangle = 0. \tag{A.4}$$

We can further characterize the fermion operators. The following rules can be derived by invoking antisymmetry of fermionic states.

$$\{c^\dagger_{\nu_j}, c^\dagger_{\nu_k}\} = 0, \; \{c_{\nu_j}, c_{\nu_k}\} = 0, \; \{c_{\nu_j}, c^\dagger_{\nu_k}\} = \delta_{jk} \tag{A.5}$$

$$c^\dagger_{\nu_j}c_{\nu_j}\,|n_{\nu_j}\rangle = n_{\nu_j}\,|n_{\nu_j}\rangle\,, \tag{A.6}$$

where n_{ν_j} is the number of particles filling the state ν_j, and can for fermions be either 0 or 1. The operator $c^\dagger_{\nu_j}c_{\nu_j}$ is sometimes refered to as the number operator of a state. Here the curly brackets denote the anticommutator of operators, and the anticommutation rules (A.5) can be used as the starting point for defining fermions.

Operators in second quantization

Operators acting on only one particle, j, can in general be represented by their matrix elements in the following way,

$$T_j = \sum_{\nu_l \nu_k} \langle \nu_l | T \nu_k \rangle \, |\nu_l\rangle \, \langle \nu_k| = \sum_{\nu_l \nu_k} T_{\nu_l, \nu_k} \, |\nu_l\rangle \, \langle \nu_k| \,, \tag{A.7}$$

where ν denotes a complete basis orthonormal basis. The above operator could for example be the kinetic energy operator, and the total kinetic energy of the system is then

$$T_{tot} = \sum_j T_j. \tag{A.8}$$

Taking an operator coupling two particles i, j, for example the potential between two electrons, one writes:

$$V_{ij} = \sum_{\nu_l \nu_k \nu_m \nu_n} \langle \nu_{l_i}, \nu_{k_j} | V \nu_{m_i}, \nu_{n_j} \rangle \, |\nu_{l_i}, \nu_{k_j}\rangle \, \langle \nu_{m_i}, \nu_{n_j}| = \sum_{\nu_l \nu_k \nu_m \nu_n} V_{\nu_l, \nu_k, \nu_m, \nu_n} \, |\nu_{l_i}, \nu_{k_j}\rangle \, \langle \nu_{m_i}, \nu_{n_j}| \,, \tag{A.9}$$

$$V_{tot} = \sum_{i,j} V_{ij} \tag{A.10}$$

enabling us to write an operator in any new basis, once it has been found in one basis.
From this, we can use the second quantization formalism to write the operators. The general idea is to construct the many-particle state function from the vacuum state using creation operators, and then use how operators act on a single particle state. The result for the kinetic and potential operators above are

$$T_{tot} = \sum_{\nu_l \nu_k} T_{\nu_l, \nu_k} c^\dagger_{\nu_l} c_{\nu_k} \tag{A.11}$$

$$V_{tot} = \sum_{\nu_l \nu_k \nu_m \nu_n} V_{\nu_l, \nu_k, \nu_m, \nu_n} c^\dagger_{\nu_l} c^\dagger_{\nu_k} c_{\nu_m} c_{\nu_n}, \tag{A.12}$$

providing an intuitive way of understanding how operators work.

Change of basis in second quantization

To change basis in the first quantization formalism one writes

$$|\mu\rangle = \sum_\nu \langle \mu | \nu \rangle^* \, |\nu\rangle \,. \tag{A.13}$$

Now, this can be written in the following way

$$c^\dagger_\mu \, |0\rangle = \sum_\nu \langle \mu | \nu \rangle^* \, c^\dagger_\nu \, |0\rangle \,, \tag{A.14}$$

which implies

$$c^\dagger_\mu = \sum_\nu \langle \mu | \nu \rangle^* \, c^\dagger_\nu, \qquad c_\mu = \sum_\nu \langle \mu | \nu \rangle \, c_\nu, \tag{A.15}$$

where the second equation comes from complex conjugating (A.13).

Real space and momentum space operators

Given real space creation/annihilation operators,

$$\Psi^\dagger(\mathbf{r}), \quad \Psi(\mathbf{r}) \tag{A.16}$$

one can write the momentum space creation/annihilation operators using the rules of change of basis:

$$c^\dagger_{\mathbf{k}} = \int d\mathbf{r} \, \langle k | r \rangle^* \, \Psi^\dagger(\mathbf{r}) = \int d\mathbf{r} e^{-\mathbf{k}\cdot\mathbf{r}} \Psi^\dagger(\mathbf{r}), \tag{A.17}$$

$$c_{\mathbf{k}} = \int d\mathbf{r} \, \langle k | r \rangle \, \Psi(\mathbf{r}) = \int d\mathbf{r} e^{\mathbf{k}\cdot\mathbf{r}} \Psi(\mathbf{r}), \tag{A.18}$$

where we used integration over $\mathbf{r}$ instead of a summation as in (A.13), as the position basis is continuous. Thus it is clear that, going from real space to momentum space in terms of creation/annihilation operators amounts to Fourier transforming the operators.

B Basics of BCS-theory

Cooper pairs

Generally, electrons interact via the coloumb interaction

$$V(\mathbf{r}-\mathbf{r}') = \frac{e^2}{4\pi\epsilon_0}\frac{1}{|\mathbf{r}-\mathbf{r}'|}. \tag{B.1}$$

In a crystal, however, electrons are in the so-called Bloch-states, modulated by the periodic structure of the crystal lattice, which, at finite temperature, is not rigid. Due to oscillations of the crystal ions, electrons scatter by means of electron-phonon interactions. These interactions affect electron-electron interaction in the crystal, and the effective interaction between electrons can, with a few assumptions, be shown to be [3]

$$H_I = -V_{eff}\sum c^\dagger_{\mathbf{k_1}+\mathbf{q},\sigma_1} c^\dagger_{\mathbf{k_2}-\mathbf{q},\sigma_2} c_{\mathbf{k_1},\sigma_1} c^\dagger_{\mathbf{k_2},\sigma_2}, \tag{B.2}$$

where the sum is over all possible values of $\mathbf{k_1}, \mathbf{k_2}, \mathbf{q}, \sigma_1, \sigma_2$ such that the electron energies involved fulfill the criteria,

$$|\epsilon_{\mathbf{k}} - \epsilon_F| < \hbar\omega_D \tag{B.3}$$

where ϵ_F is the Fermi-energy and ω_D is the Debye-frequency. Here we have assumed that V_{eff} is independent of the spin and momenta of the annihilated and created electrons, although this is not generally the case.
It was shown by Cooper that this interaction leads to a bound state between electrons of opposite momentum in states above a filled Fermi sea. The observation of Cooper pairs are central to the understanding of BCS superconductivity.

Mean-field Hamiltonian of the superconducting state

Using the effective interactions between electrons in the superconductor (B.2), the Hamiltonian of the system is:

$$\begin{aligned} H &= \sum_{\mathbf{k}\sigma}(\epsilon_{\mathbf{k}}-\mu)c^\dagger_{\mathbf{k}\sigma}c_{\mathbf{k}\sigma} - V_{eff}\sum c^\dagger_{\mathbf{k_1}+\mathbf{q},\sigma_1} c^\dagger_{\mathbf{k_2}-\mathbf{q},\sigma_2} c_{\mathbf{k_1},\sigma_1} c_{\mathbf{k_2},\sigma_2} \\ &= \sum_{\mathbf{k}\sigma}(\epsilon_{\mathbf{k}}-\mu)c^\dagger_{\mathbf{k}\sigma}c_{\mathbf{k}\sigma} - V_{eff}\sum_{\mathbf{k}\mathbf{k}'} c^\dagger_{\mathbf{k},\uparrow} c^\dagger_{-\mathbf{k},\downarrow} c_{\mathbf{k}',\uparrow} c_{-\mathbf{k}',\downarrow}, \end{aligned} \tag{B.4}$$

where, in the second equality, we assume that only scatterings of Cooper pairs into other Cooper pairs are important. This amounts to assuming that we are in a temperature range, where the bound states cannot be broken by thermal excitations. We now make the mean-field appromixation

$$c^\dagger_{\mathbf{k},\uparrow} c^\dagger_{-\mathbf{k},\downarrow} c_{\mathbf{k}',\uparrow} c_{-\mathbf{k}',\downarrow} \approx \langle c^\dagger_{\mathbf{k},\uparrow} c^\dagger_{-\mathbf{k},\downarrow}\rangle c_{\mathbf{k}',\uparrow} c_{-\mathbf{k}',\downarrow} + c^\dagger_{\mathbf{k},\uparrow} c^\dagger_{-\mathbf{k},\downarrow} \langle c_{\mathbf{k}',\uparrow} c_{-\mathbf{k}',\downarrow}\rangle . \tag{B.5}$$

Defining,

$$\Delta = -V_{eff}\sum_{\mathbf{k}} \langle c_{-\mathbf{k},\downarrow} c_{\mathbf{k},\uparrow}\rangle , \tag{B.6}$$

we can rewrite (B.4) into

$$\begin{aligned} H &= \sum_{\mathbf{k}\sigma}(\epsilon_{\mathbf{k}}-\mu)c^\dagger_{\mathbf{k}\sigma}c_{\mathbf{k}\sigma} + \sum_{\mathbf{k}} \Delta c^\dagger_{\mathbf{k},\uparrow} c^\dagger_{-\mathbf{k},\downarrow} + \Delta^* c_{-\mathbf{k},\downarrow} c_{\mathbf{k},\uparrow} \\ &= \sum_{\mathbf{k}} \begin{pmatrix} c^\dagger_{\mathbf{k},\uparrow} & c_{-\mathbf{k},\downarrow} \end{pmatrix} \begin{pmatrix} (\epsilon_{\mathbf{k}}-\mu) & \Delta \\ \Delta^* & -(\epsilon_{\mathbf{k}}-\mu) \end{pmatrix} \begin{pmatrix} c_{\mathbf{k},\uparrow} \\ c^\dagger_{-\mathbf{k},\downarrow} \end{pmatrix} + (\epsilon_{\mathbf{k}}-\mu), \end{aligned} \tag{B.7}$$

where in the second equality we make use of the fermion anticommutation relations, something that will be made more explicit in section 3. The constant term can be absorbed in the definition of the Hamiltonian and thus we refrain from writing it from now on. Now introduce the unitary matrix,

$$U = \begin{pmatrix} u_{\mathbf{k}} & v_{\mathbf{k}}^* \\ -v_{\mathbf{k}} & u_{\mathbf{k}}^* \end{pmatrix} \tag{B.8}$$

and demand that it diagonalizes the 2-by-2 matrix in (B.7)

$$\begin{aligned} U^\dagger \mathcal{H} U &= \begin{pmatrix} u_{\mathbf{k}}^* & -v_{\mathbf{k}}^* \\ v_{\mathbf{k}} & u_{\mathbf{k}} \end{pmatrix} \begin{pmatrix} (\epsilon_{\mathbf{k}} - \mu) & \Delta \\ \Delta^* & -(\epsilon_{\mathbf{k}} - \mu) \end{pmatrix} \begin{pmatrix} u_{\mathbf{k}} & v_{\mathbf{k}}^* \\ -v_{\mathbf{k}} & u_{\mathbf{k}}^* \end{pmatrix} \\ &= \begin{pmatrix} E_{\mathbf{k}} & 0 \\ 0 & -E_{\mathbf{k}} \end{pmatrix}, \end{aligned} \tag{B.9}$$

with the eigenenergies

$$E_{\mathbf{k}} = \pm\sqrt{(\epsilon_{\mathbf{k}} - \mu)^2 + |\Delta|^2}. \tag{B.10}$$

This, together with the unitarity of U imposes the following constraints on $u_{\mathbf{k}}$ and $v_{\mathbf{k}}$:

$$2u_{\mathbf{k}} v_{\mathbf{k}} (\epsilon_{\mathbf{k}} - \mu) + \Delta^* u_{\mathbf{k}}^2 - \Delta v_{\mathbf{k}}^2 = 0, \tag{B.11}$$

$$|u_{\mathbf{k}}|^2 + |v_{\mathbf{k}}|^2 = 1. \tag{B.12}$$

Multiplying through (B.11) by respectively $\frac{\Delta}{u_{\mathbf{k}^2}}$ and $\frac{\Delta^*}{v_{\mathbf{k}^2}}$ and solving for respectively $\frac{\Delta v_{\mathbf{k}}}{u_{\mathbf{k}}}$ and $\frac{\Delta^* u_{\mathbf{k}}}{v_{\mathbf{k}}}$,

$$u_{\mathbf{k}}(\epsilon_{\mathbf{k}} - \mu) + \Delta v_{\mathbf{k}} = E_{\mathbf{k}} u_{\mathbf{k}}, \tag{B.13}$$

$$-v_{\mathbf{k}}(\epsilon_{\mathbf{k}} - \mu) + \Delta^* u_{\mathbf{k}} = E_{\mathbf{k}} v_{\mathbf{k}}. \tag{B.14}$$

In this basis we can thus write the Hamiltonian as:

$$H = \sum_{\mathbf{k}} \begin{pmatrix} \gamma_{\mathbf{k}\uparrow}^\dagger & \gamma_{-\mathbf{k}\downarrow} \end{pmatrix} \begin{pmatrix} E_{\mathbf{k}} & 0 \\ 0 & -E_{\mathbf{k}} \end{pmatrix} \begin{pmatrix} \gamma_{\mathbf{k}\uparrow} \\ \gamma_{-\mathbf{k}\downarrow}^\dagger \end{pmatrix} = \sum_{\mathbf{k}} E_{\mathbf{k}} (\gamma_{\mathbf{k}\uparrow}^\dagger \gamma_{\mathbf{k}\uparrow} - \gamma_{-\mathbf{k}\downarrow} \gamma_{-\mathbf{k}\downarrow}^\dagger) \tag{B.15}$$

with

$$\gamma_{\mathbf{k}\uparrow}^\dagger = c_{\mathbf{k},\uparrow}^\dagger u_{\mathbf{k}} - c_{-\mathbf{k},\downarrow} v_{\mathbf{k}}, \tag{B.16}$$

$$\gamma_{-\mathbf{k}\downarrow} = c_{\mathbf{k},\uparrow}^\dagger v_{\mathbf{k}}^* + c_{-\mathbf{k},\downarrow} u_{\mathbf{k}}^*. \tag{B.17}$$

The preceeding transformation of the Hamiltonian is called a Bogoliubov transformation. The result suggests that in the superconducting state the relevant excitation particles are neither electrons or holes, but superpositions of these. One can show that these excitation particles are fermions which are not present in the BCS ground state.

C Second quantization of Rashba spin-orbit Hamiltonian in 2D

The spin-orbit coupling term of the Hamiltonian is:

$$H_{so} = \frac{\mu_B}{4mc^2} (\mathbf{p} \times \mathbf{E}) \cdot \boldsymbol{\sigma}. \tag{C.1}$$

To bind electrons in three dimensions to a two dimensional crystal lattice, say in the x,- and y-directions, one could imagine an E-field in the z-direction, $\mathbf{E} = -\frac{\partial V}{\partial z} \mathbf{e}_{\hat{\mathbf{z}}}$, where V is the electrical potential. Inserting this in the spin orbit Hamiltonian, we obtain:

$$H_{so} = \frac{\partial V}{\partial z} \frac{\mu_B}{4mc^2} (\mathbf{e}_{\hat{\mathbf{z}}} \times \mathbf{p}) \cdot \boldsymbol{\sigma} = \gamma (p_x \sigma_y - p_y \sigma_x), \tag{C.2}$$

which is the so called Rashba spin-orbit Hamiltonian. We wish to write this in a 2. quantized form with creation-annihilation operators (c.a.o) corresponding to atomic orbitals in our 2D-lattice:

$$H_{so} = \sum_{i,j} \sum_{\sigma,\sigma'} \gamma \int d^3\mathbf{r} \varphi^*(\mathbf{r} - \mathbf{R}_i) \chi_\sigma (p_x \sigma_y - p_y \sigma_x) \chi_{\sigma'} \varphi(\mathbf{r} - \mathbf{R}_j) c_{i\sigma}^\dagger c_{j\sigma'}, \tag{C.3}$$

where $\mathbf{R}_i$ denotes the i'th lattice site, σ and σ' denote the spin orientation in the z-direction, χ is the electron spin-state and $\varphi(\mathbf{r})$ is an atomic orbital. We assume only one kind of orbital can be occupied, say, the orbital of quantum numbers (nlm). Letting the Pauli-matrices operate on the spin-state we obtain:

$$H_{so} = \sum_{i,j} \sum_{\sigma,\sigma'} \gamma \int d^3\mathbf{r} \varphi^*(\mathbf{r} - \mathbf{R}_i)(p_x \sigma^{(y)}_{\sigma,\sigma'} - p_y \sigma^{(x)}_{\sigma,\sigma'}) \varphi(\mathbf{r} - \mathbf{R}_j) c^\dagger_{i\sigma} c_{j\sigma'}. \tag{C.4}$$

Now, we wish to find the effect of p_x,p_y on the orbital wave functions. In a crystal lattice, the derivative of a function must be defined as a difference, with the smallest distance between two points of the function being the lattice constant a, i.e., we write:

$$\frac{\partial}{\partial x} f(\mathbf{r}) = \frac{1}{2}\left(\frac{f(\mathbf{r} + a\hat{x}) - f(\mathbf{r})}{a} - \frac{f(\mathbf{r} - a\hat{x}) - f(\mathbf{r})}{a} \right) = \frac{1}{2}\left(\frac{f(\mathbf{r} + a\hat{x}) - f(\mathbf{r} - a\hat{x})}{a} \right). \tag{C.5}$$

Setting $a = 1$, we can write the integrand of the Hamiltonian:

$$\frac{\hbar}{2i} \varphi^*(\mathbf{r} - \mathbf{R}_i) \left(\left[\varphi(\mathbf{r} - \mathbf{R}_j + \hat{x}) - \varphi(\mathbf{r} - \mathbf{R}_j - \hat{x}) \right] \sigma^{(y)}_{\sigma,\sigma'} - \left[\varphi(\mathbf{r} - \mathbf{R}_j + \hat{y}) - \varphi(\mathbf{r} - \mathbf{R}_j - \hat{y}) \right] \sigma^{(x)}_{\sigma,\sigma'} \right). \tag{C.6}$$

We now demand that

$$\int d^3\mathbf{r} \varphi^*(\mathbf{r} - \mathbf{R}_i) \varphi(\mathbf{r} - \mathbf{R}_j) = \delta_{ij}, \tag{C.7}$$

that is, we assume that the atomic orbitals are well localized around their respective crystal sites. With this assumption, the Hamiltonian becomes:

$$\begin{aligned} H_{so} &= \frac{\gamma\hbar}{2i} \sum_j \sum_{\sigma,\sigma'} \left(c^\dagger_{j\sigma} \sigma^{(y)}_{\sigma,\sigma'} c_{j-\delta_x\sigma'} - c^\dagger_{j\sigma} \sigma^{(y)}_{\sigma,\sigma'} c_{j+\delta_x\sigma'} - c^\dagger_{j\sigma} \sigma^{(x)}_{\sigma,\sigma'} c_{j-\delta_y\sigma'} + c^\dagger_{j\sigma} \sigma^{(x)}_{\sigma,\sigma'} c_{j+\delta_y\sigma'} \right) \\ &= -\frac{\gamma\hbar}{2} \sum_j \sum_{\sigma,\sigma'} i \left(c^\dagger_{j\sigma} \sigma^{(y)}_{\sigma,\sigma'} c_{j-\delta_x\sigma'} - c^\dagger_{j\sigma} \sigma^{(y)}_{\sigma,\sigma'} c_{j+\delta_x\sigma'} - c^\dagger_{j\sigma} \sigma^{(x)}_{\sigma,\sigma'} c_{j-\delta_y\sigma'} + c^\dagger_{j\sigma} \sigma^{(x)}_{\sigma,\sigma'} c_{j+\delta_y\sigma'} \right). \end{aligned}$$

Here $j \pm \delta_{x,y}$ denote the site closest to site j in either x or y directions. We can write this in another form:

$$\begin{aligned} H_{so} &= -\frac{\gamma\hbar}{2} \sum_j \sum_{\sigma,\sigma'} i \left(c^\dagger_{j\sigma} \sigma^{(x)}_{\sigma,\sigma'} c_{j+\delta_y\sigma'} - c^\dagger_{j\sigma} \sigma^{(y)}_{\sigma,\sigma'} c_{j+\delta_x\sigma'} + c^\dagger_{j\sigma} \sigma^{(y)}_{\sigma,\sigma'} c_{j-\delta_x\sigma'} - c^\dagger_{j\sigma} \sigma^{(x)}_{\sigma,\sigma'} c_{j-\delta_y\sigma'} \right) \\ &= -\frac{\gamma\hbar}{2} \sum_j \sum_{\sigma,\sigma'} i \left(c^\dagger_{j\sigma} \sigma^{(x)}_{\sigma,\sigma'} c_{j+\delta_y\sigma'} - c^\dagger_{j\sigma} \sigma^{(y)}_{\sigma,\sigma'} c_{j+\delta_x\sigma'} + c^\dagger_{j+\delta_x\sigma} \sigma^{(y)}_{\sigma,\sigma'} c_{j\sigma'} - c^\dagger_{j+\delta_y\sigma} \sigma^{(x)}_{\sigma,\sigma'} c_{j\sigma'} \right), \end{aligned}$$

which we recognize as a sum and its hermitian conjugate. In the last equality we invoke periodic boundary conditions, and rewrite the summing index to $j' = j - \delta_{x,y}$, and obtain the form written above. We denote $E_{so} = \frac{\gamma\hbar}{2}$, and write out the Rashba Hamiltonian:

$$\begin{aligned} H_{so} = -E_{so} \sum_j & i(c^\dagger_{j\uparrow} c_{j+\delta_y\downarrow} + c^\dagger_{j\downarrow} c_{j+\delta_y\uparrow}) + (-c^\dagger_{j\uparrow} c_{j+\delta_x\downarrow} + c^\dagger_{j\downarrow} c_{j+\delta_x\uparrow}) \\ & - i(c^\dagger_{j+\delta_y\uparrow} c_{j\downarrow} + c^\dagger_{j+\delta_y\downarrow} c_{j\uparrow}) - (-c^\dagger_{j+\delta_x\uparrow} c_{j\downarrow} + c^\dagger_{j+\delta_x\downarrow} c_{j\uparrow}). \end{aligned} \tag{C.8}$$

We now change basis from real space to k-space, using:

$$c_{i\sigma} = \frac{1}{N} \sum_{\mathbf{k}} e^{\mathbf{k}\cdot\mathbf{r}_i} c_{\mathbf{k}\sigma}. \tag{C.9}$$

Denoting the two terms in the Hamiltonian, in which an i-factor is present, (1) and the other two terms (2) we obtain in the k-basis:

$$(1) = -\frac{E_{so}}{N^2} \sum_j \sum_{\mathbf{k},\mathbf{k}'} i \left(e^{i(\mathbf{k}-\mathbf{k}')\cdot\mathbf{r}_j} \left(e^{ik_y} (c^\dagger_{\mathbf{k}'\uparrow} c_{\mathbf{k}\downarrow} + c^\dagger_{\mathbf{k}'\downarrow} c_{\mathbf{k}\uparrow}) - e^{-ik'_y} (c^\dagger_{\mathbf{k}'\uparrow} c_{\mathbf{k}\downarrow} + c^\dagger_{\mathbf{k}'\downarrow} c_{\mathbf{k}\uparrow}) \right) \right)$$

$$= -E_{so} \sum_{\mathbf{k}} -2\sin(k_y)(c^\dagger_{\mathbf{k}\uparrow} c_{\mathbf{k}\downarrow} + c^\dagger_{\mathbf{k}\downarrow} c_{\mathbf{k}\uparrow}),$$

$$(2) = -\frac{E_{so}}{N^2} \sum_j \sum_{\mathbf{k},\mathbf{k}'} \left(e^{i(\mathbf{k}-\mathbf{k}')\cdot \mathbf{r}_j} \left(e^{ik_x}(-c^\dagger_{\mathbf{k}'\uparrow} c_{\mathbf{k}\downarrow} + c^\dagger_{\mathbf{k}'\downarrow} c_{\mathbf{k}\uparrow}) - e^{-ik'_x}(-c^\dagger_{\mathbf{k}'\uparrow} c_{\mathbf{k}\downarrow} + c^\dagger_{\mathbf{k}'\downarrow} c_{\mathbf{k}\uparrow}) \right) \right)$$

$$= -E_{so} \sum_{\mathbf{k}} i2\sin(k_x)(-c^\dagger_{\mathbf{k}\uparrow} c_{\mathbf{k}\downarrow} + c^\dagger_{\mathbf{k}\downarrow} c_{\mathbf{k}\uparrow}),$$

where we have used

$$\sum_j \sum_{\mathbf{k},\mathbf{k}'} e^{i(\mathbf{k}-\mathbf{k}')\cdot \mathbf{r}_j} = \sum_j \sum_{\mathbf{k},\mathbf{k}'} \delta_{\mathbf{k},\mathbf{k}'} = N^2 \sum_{\mathbf{k}}.$$

D Explicit calculation of the Berry phase

Consider a time dependent Hamiltonian and its eigenstates $\psi_n(t)$,

$$H(t)\psi_n(t) = E_n(t)\psi_n(t), \tag{D.1}$$

where we demand that the set of eigenstates evolve such that at each t they consitute a orthonormal and complete set. We also assume they are non-degenerate. We then make the following ansatz about the general solution to the Schrödinger equation;

$$i\hbar \frac{\partial}{\partial t}\Psi(t) = H(t)\Psi(t) \tag{D.2}$$

$$\Psi(t) = \sum_n c_n(t)\psi_n(t)e^{i\theta_n(t)}, \tag{D.3}$$

that is, any solution to the Schrödinger equation can be expressed as a linear combination of the momentary eigenstates of $H(t)$. Here,

$$\theta_n(t) = -\frac{1}{\hbar}\int_0^t E_n(t')dt' \tag{D.4}$$

is simply the generalization of the dynamical phase one would obtain by solving for the time independent Schrödinger equation. Inserting the ansatz into the Schrödinger equation we obtain the equation,

$$\begin{aligned} i\hbar \sum_n \dot{c_n}\psi_n e^{i\theta_n} + c_n\dot{\psi_n}e^{i\theta_n} + ic_n\psi_n\dot{\theta}_n e^{i\theta_n} &= H(t)\sum_n c_n\psi_n e^{i\theta_n} \\ &= \sum_n c_n E_n \psi_n e^{i\theta_n} \\ \implies \sum_n \dot{c_n}\psi_n e^{i\theta_n} + c_n\dot{\psi_n}e^{i\theta_n} &= 0, \end{aligned}$$

where we have used (D.4) and (D.1). Using orthonormality of the eigenstates we can write,

$$\dot{c}_m = -\sum_n c_n \langle \psi_m | \dot{\psi_n} \rangle e^{i(\theta_n - \theta_m)}. \tag{D.5}$$

Now, differentiating (D.1) and taking the inner product of this equation with two eigenstates we obtain the expression

$$\frac{\langle \psi_m | \dot{H} | \psi_n \rangle}{E_m - E_n} = \langle \psi_m | \dot{\psi_n} \rangle, \tag{D.6}$$

if $n \neq m$. Using this in (D.5) we can write

$$\begin{aligned} \dot{c}_m &= -c_m \langle \psi_m | \dot{\psi_m} \rangle - \sum_{n\neq m} c_n \frac{\langle \psi_m | \dot{H} | \psi_n \rangle}{E_m - E_n} e^{i(\theta_n - \theta_m)} \approx -c_m \langle \psi_m | \dot{\psi_m} \rangle \\ \implies c_m(t) &= c_m(0) e^{-\int_0^t \langle \psi_m(t') | \dot{\psi}(t')_m \rangle dt'} \end{aligned}$$

where in the appromixation step we assumed that H is only slowly varying, which is usually called the adiabatic approximation (here adiabatic is in stark contrast to its meaning in thermodynamics.). Thus we finally have arrived at an expression for the general solution to the Schrödinger equation,

$$\Psi(t) = \sum_n \psi_n(t) e^{i(\theta_n(t)+\gamma_n(t))}, \tag{D.7}$$

where $\gamma_n(t) = i\int_0^t \langle\psi_m(t')|\dot{\psi}_m(t')\rangle\, dt'$ is called the geometric phase. Now imagine that the Hamiltonian is dependent on t through a set of parameters P_n,

$$H(P_1(t), P_2(t), ..., P_N(t)). \tag{D.8}$$

Then the eigenstates of the Hamiltonian only depend on t through P_n, thus enabling us to write,

$$\frac{d\psi_n}{dt} = \frac{\partial\psi_n}{\partial P_i}\frac{dP_i}{dt}, \tag{D.9}$$

which further implies that,

$$\gamma_n(t) = i\int_0^t \langle\psi_n(t')|\dot{\psi}_m(t')\rangle\, dt' = i\int_{\mathbf{P}_0}^{\mathbf{P}_1} \langle\psi_n|\frac{\partial\psi_n}{\partial P_i}\rangle\, d\mathbf{P}. \tag{D.10}$$

where the integral is now over coordinates of a curve in the N'th dimensional parameter space and $\mathbf{P}_0$ and $\mathbf{P}_1$ are the endpoints of the curve. We mention that here $\frac{\partial}{\partial P_i}$ denotes the gradient operator in parameter space. If now the two endpoints of curve are the same point then,

$$\gamma_n(t) = i\oint \langle\psi_n|\frac{\partial\psi_n}{\partial P_i}\rangle\, d\mathbf{P}, \tag{D.11}$$

i.e. the integral is over a closed curve, and is generally not zero. This is called the Berry phase and has measureable consequences.
When the parameter space is only 3 dimensional it can be shown through the regular Stokes' theorem from vector calculus that,

$$\gamma_n = i\oint \langle\psi_n|\frac{\partial\psi_n}{\partial P_i}\rangle\, d\mathbf{P} = i\int_S \nabla\times\langle\psi_n|\frac{\partial\psi_n}{\partial P_i}\rangle\cdot d\mathbf{a} \equiv i\int_S \mathbf{B}_n\cdot d\mathbf{a}, \tag{D.12}$$

and that,

$$\mathbf{B}_n = i\sum_{m\neq n}\frac{\langle\psi_n|\nabla H|\psi_m\rangle\times\langle\psi_m|\nabla H|\psi_n\rangle}{(E_n-E_m)^2}, \tag{D.13}$$

emphasizing that the non-degeneracy of the eigenstates has been assumed. $\mathbf{B}_n$ is usually called the Berry curvature, and for completeness we mention that usually,

$$\langle\psi_n|\frac{\partial\psi_n}{\partial P_i}\rangle \equiv \mathbf{A}_n, \tag{D.14}$$

is called the Berry connection.

E Low energy states vs. external magnetic field

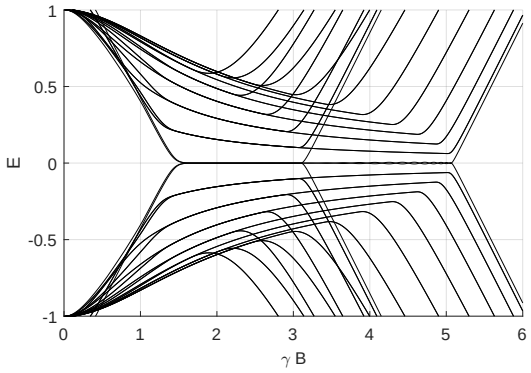

(a)

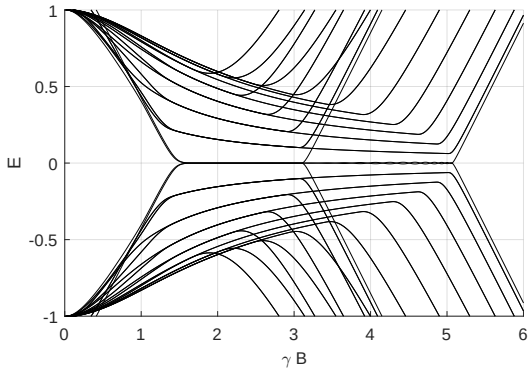

(b)

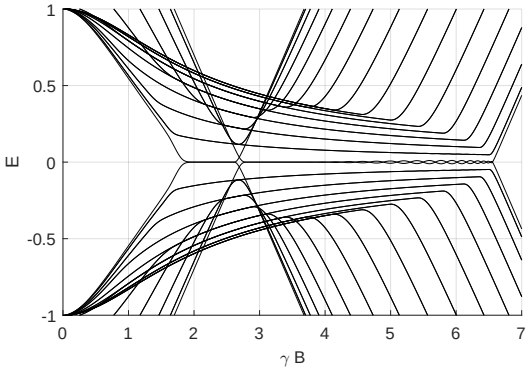

(c)

Figure 15: Lowest energy states for (a) $\mu = -1$ ($-2t < \mu \leq 0$), bulk gap closings at $\gamma B = (1.41, 3.16, 5.1)$. (b) $\mu = 1$ ($0 < \mu \leq 2t$), bulk gap closings same as in (a). (c) $\mu = 2.5$ ($2t < \mu$), bulk gap closings at $\gamma B = (1.80, 2.69, 6.58)$.

F Zero-energy state in the semi-periodic lattice

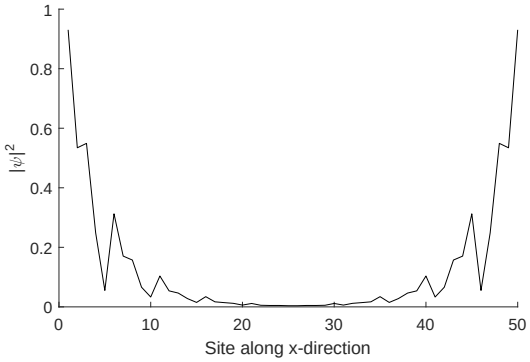

Figure 16: The wavefunction for a Majorana state with $k_y = 0$ at $\gamma B = 2$. The state is confined to both the edges, as was the case in the 1D system.

G LDOS in the semi-periodic lattice in the trivial phase

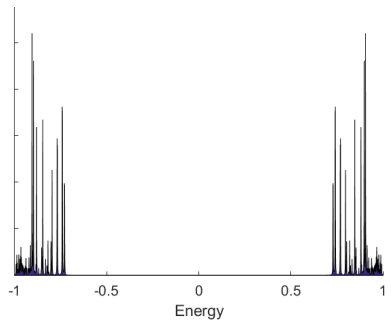

(a) Site number 1 in the x-direction (edge site)

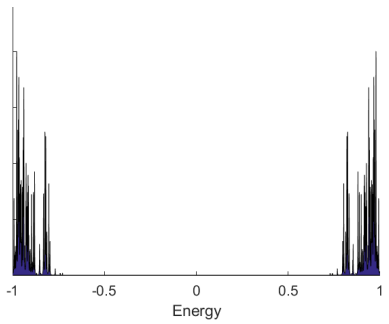

(b) Site number 15 in the x-direction (bulk site)

Figure 17: In the trivial regime; LDOS at an edge site and at a bulk site. $\gamma B = 0.7$, all other parameters as in the non-trivial case

H LDOS around a vortex in the trivial phase

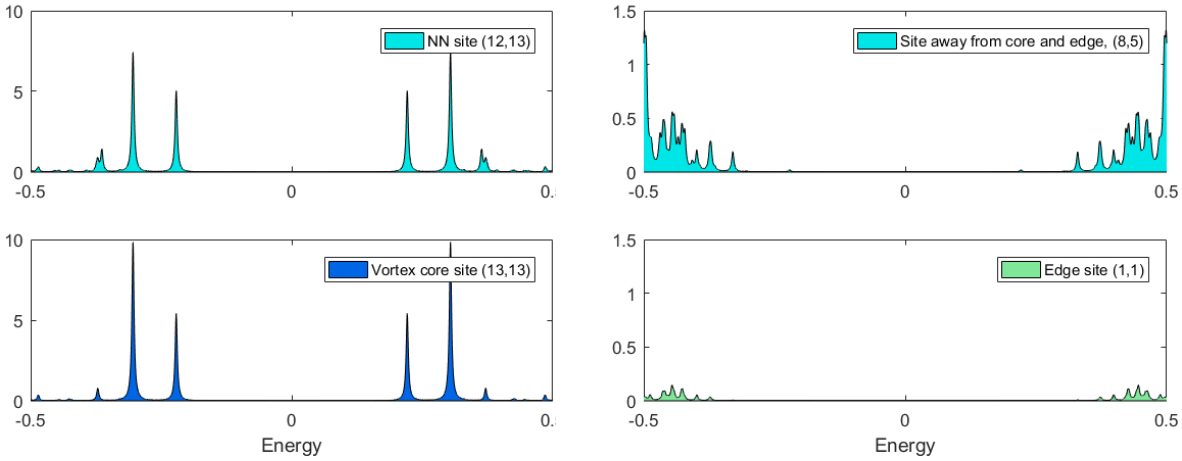

(a) (b)

Figure 18: In the trivial regime; (a) LDOS at the vortex core and a nearest neighbor site and (b) at a site away from the core and the edge of the lattice and at an edge site. $\gamma B = 0.2$ all other parameters as in the non-trivial case.

I Explicit calculation of the BdG Hamiltonian in k-space

Starting from the Hamiltonian (5.1) we use the fermionic commutation relations to obtain

$$\begin{aligned} H &= \frac{1}{2}\sum_{\mathbf{k},\sigma,\sigma'}\left(-\epsilon(\mathbf{k})\mathbb{I}_{\sigma,\sigma'} - \gamma B\sigma^{(z)}_{\sigma,\sigma'} + \mathbf{E}_{so}(\mathbf{k})\cdot\boldsymbol{\sigma}_{\sigma,\sigma'}\right)\left(c^\dagger_{\mathbf{k}\sigma}c_{\mathbf{k}\sigma'} - c_{\mathbf{k}\sigma'}c^\dagger_{\mathbf{k}\sigma}\right) \\ &+\frac{1}{2}\sum_{\mathbf{k}}\Delta(\mathbf{k})\left(c^\dagger_{\mathbf{k}\uparrow}c^\dagger_{-\mathbf{k}\downarrow} - c^\dagger_{-\mathbf{k}\downarrow}c^\dagger_{\mathbf{k}\uparrow}\right) + \Delta^*(\mathbf{k})\left(c_{-\mathbf{k}\downarrow}c_{\mathbf{k}\uparrow} - c_{\mathbf{k}\uparrow}c_{-\mathbf{k}\downarrow}\right) + \text{const.} \\ &= \frac{1}{2}\sum_{\mathbf{k},\sigma,\sigma'}\left(-\epsilon(\mathbf{k})\mathbb{I}_{\sigma,\sigma'} - \gamma B\sigma^{(z)}_{\sigma,\sigma'} + \mathbf{E}_{so}(\mathbf{k})\cdot\boldsymbol{\sigma}_{\sigma,\sigma'}\right)\left(c^\dagger_{\mathbf{k}\sigma}c_{\mathbf{k}\sigma'} - c_{\mathbf{k}\sigma'}c^\dagger_{\mathbf{k}\sigma}\right) \\ +\frac{1}{2}\sum_{\mathbf{k}}&\left(\Delta(\mathbf{k})c^\dagger_{\mathbf{k}\uparrow}c^\dagger_{-\mathbf{k}\downarrow} + \Delta^*(\mathbf{k})c_{-\mathbf{k}\downarrow}c_{\mathbf{k}\uparrow}\right) - \left(\Delta(-\mathbf{k})c^\dagger_{\mathbf{k}\downarrow}c^\dagger_{-\mathbf{k}\uparrow} + \Delta^*(-\mathbf{k})c_{-\mathbf{k}\uparrow}c_{\mathbf{k}\downarrow}\right) + \text{const.} \end{aligned} \tag{I.1}$$

Throwing away the constant terms and using the Nambu-vectors, we can write this Hamiltonian as

$$\begin{pmatrix} -2t(\cos(k_x)+\cos(k_y))-\mu-\gamma B & E_{so}(\sin(k_y)+i\sin(k_x)) & 0 & \Delta(\mathbf{k}) \\ E_{so}(\sin(k_y)-i\sin(k_x)) & -2t(\cos(k_x)+\cos(k_y))-\mu+\gamma B & -\Delta(-\mathbf{k}) & 0 \\ 0 & -\Delta^*(-\mathbf{k}) & 2t(\cos(-k_x)+\cos(-k_y))+\mu+\gamma B & -E_{so}(\sin(-k_y)-i\sin(-k_x)) \\ \Delta^*(\mathbf{k}) & 0 & -E_{so}(\sin(-k_y)+i\sin(-k_x)) & 2t(\cos(-k_x)+\cos(-k_y))+\mu-\gamma B \end{pmatrix}, \tag{I.2}$$

where the Nambu-vectors on each side of the matrix is implied.
To realize this one should do the matrix product with the Nambu-vectors, which we do here with the second and fourth quadrant. First let us write the product due to the second quadrant:

$$\begin{aligned} \begin{pmatrix} c^\dagger_{\mathbf{k}\uparrow} & c^\dagger_{\mathbf{k}\downarrow} \end{pmatrix}\begin{pmatrix} 0 & \Delta(\mathbf{k}) \\ -\Delta(-\mathbf{k}) & 0 \end{pmatrix}\begin{pmatrix} c^\dagger_{-\mathbf{k}\uparrow} \\ c^\dagger_{-\mathbf{k}\downarrow} \end{pmatrix} &= \sum_{\mathbf{k}}\Delta(\mathbf{k})c^\dagger_{\mathbf{k}\uparrow}c^\dagger_{-\mathbf{k}\downarrow} - \Delta(-\mathbf{k})c^\dagger_{\mathbf{k}\downarrow}c^\dagger_{-\mathbf{k}\uparrow} \\ &= \sum_{\mathbf{k}}\Delta(\mathbf{k})c^\dagger_{\mathbf{k}\uparrow}c^\dagger_{-\mathbf{k}\downarrow} - \Delta(\mathbf{k})c^\dagger_{-\mathbf{k}\downarrow}c^\dagger_{\mathbf{k}\uparrow}, \end{aligned} \tag{I.3}$$

which is also what appears in the sum of the Hamiltonian. Next we do the fourth quadrant:

$$\begin{aligned}
&\begin{pmatrix} c_{-\mathbf{k}\uparrow} & c_{-\mathbf{k}\downarrow} \end{pmatrix} \begin{pmatrix} 2t(\cos(-k_x)+\cos(-k_y))+\mu+\gamma B & -E_{so}(\sin(-k_y)-i\sin(-k_x)) \\ -E_{so}(\sin(-k_y)+i\sin(-k_x)) & 2t(\cos(-k_x)+\cos(-k_y))+\mu-\gamma B \end{pmatrix} \begin{pmatrix} c^\dagger_{-\mathbf{k}\uparrow} \\ c^\dagger_{-\mathbf{k}\downarrow} \end{pmatrix} \\
&= \begin{pmatrix} c_{\mathbf{k}\uparrow} & c_{\mathbf{k}\downarrow} \end{pmatrix} \begin{pmatrix} 2t(\cos(k_x)+\cos(k_y))+\mu+\gamma B & -E_{so}(\sin(k_y)-i\sin(k_x)) \\ -E_{so}(\sin(k_y)+i\sin(k_x)) & 2t(\cos(k_x)+\cos(k_y))+\mu-\gamma B \end{pmatrix} \begin{pmatrix} c^\dagger_{\mathbf{k}\uparrow} \\ c^\dagger_{\mathbf{k}\downarrow} \end{pmatrix} \\
&= \frac{1}{2}\sum_{\mathbf{k}\sigma\sigma'} \left(-\epsilon(\mathbf{k})\mathbb{I}_{\sigma,\sigma'} - \gamma B \sigma^{(z)}_{\sigma,\sigma'} + \mathbf{E}_{so}(\mathbf{k})\cdot\boldsymbol{\sigma}_{\sigma,\sigma'} \right) \left(c^\dagger_{\mathbf{k}\sigma} c_{\mathbf{k}\sigma'} - c_{\mathbf{k}\sigma'} c^\dagger_{\mathbf{k}\sigma} \right),
\end{aligned} \tag{I.4}$$

and make the same conclusion.

J Example of the Matlab scripts used in the thesis

In the link
https://www.dropbox.com/sh/zl6xclvj2wddupq/AABawxgRMqWSalWdMajgq5iIa?dl=0
all the relevant scripts made during the project have been put up.

```
clear all
close all
clc

%This sub-script is working with a lattice assuming periodic boundaries

%N: the number of lattice sites
%t: hopping parameter
%ts: Rashba parameter
%c1 and c2: the real and imaginary parts of the superconducting gap
%s and p: the superconducting gap and its conjugate
%V: The squared modulus of the superconducting gap
%z: Zeemann parameter
%u: chemical potential
%T: Temperature
%Vsc: The effective potential coupling cooper pairs.

N=11;
t=1;
c1=1;
c2=0;
s=c1+1i*c2;
p=conj(s);
V=s*p;
u=10;
Vsc=0;
T=0.01*t;

fd = @(x) 1/(exp(x/T)+1);


%The script is essentially the making of the real space hamiltonian of
%the electrons in a specific atomic orbit of a 2D quadratic crystal
%lattice, in which is included hopping, Rashba s.o., superconductivity and
%Zeemann from an external B-field.
%We create a 4*N*N x 4*N*N matrix in terms of creation and annihilation of
%electrons in certain lattice sites with certain spins. It is 4*N*N since
%there exists coupling between both different sites and different spins.

```

```
D=10; %The number of iterations for calculating the superconducting gap self-consistently.
for d=1:D

L=10;   %The number of iterations for calculating the electron density expectation value.
for l=1:L
A=zeros((4*N*N));
%We first determine the entries due to tight-binding hopping:
for i=1:N*N                             %i denotes lattice site
    for k=1:N-2
            if i==1+k*N                 %Choose all non-corner edge-sites in the left side of the lattice
                A(i,i+1)=-t;            %Site to the right
                A(i,i-N)=-t;            %Site above
                A(i,i+N)=-t;            %Below
                A(i,i-1+N)=-t;          %"To the left" (P.B.C).

            elseif i==1+k               %Chooses all non corner edge sites in the top s.o.l.
                A(i,i+1)=-t;            %Right
                A(i,i-1)=-t;            %Left
                A(i,i+N)=-t;            %Below
                A(i,i+N*(N-1))=-t;      %"Above"

            elseif i==N+k*N             %Chooses all non corner edge sites on the right s.o.l.
                A(i,i-1)=-t;
                A(i,i+N)=-t;
                A(i,i-N)=-t;
                A(i,i-(N-1))=-t;
            elseif i==N*(N-1)+1+k               %Chooses all non-corner edge sites on the bottom s.o.l.
                A(i,i+1)=-t;
                A(i,i-1)=-t;
                A(i,i-N)=-t;
                A(i,i-N*(N-1))=-t;
            elseif i==1                         %The next four "elseifs" are for the four corners of the lattice
                A(i,i+1)=-t;
                A(i,N)=-t;
                A(i,i+N)=-t;
                A(i,i+N*(N-1))=-t;
            elseif i==N
                A(i,i-1)=-t;
                A(i,i-(N-1))=-t;
                A(i,i+N)=-t;
                A(i,N*N)=-t;
            elseif i==N*(N-1)+1
                A(i,i+1)=-t;
                A(i,i-N)=-t;
                A(i,N*N)=-t;
                A(i,1)=-t;
            elseif i==N*N
                A(i,i-1)=-t;
                A(i,i-N*(N-1))=-t;
                A(i,i-N)=-t;
                A(i,i-(N-1))=-t;
```

```
91              end
92      end
93  end
94  %Next we include the Rashba spin orbit entries:
95  for j=1:N*N             %We choose the first N*N rows, i.e. find from which
        sites spin down electrons jump and become spin up
96          if          A(j,:)==zeros(1,4*N*N) & j>=N+1 & j<=N*(N-1)+1   %This
                last line chooses the rows that still have not been filled, i.e.
                the sites in the bulk
97
98                      A(j,j-1)=-t;
99                      A(j,j+1)=-t;
100                     A(j,j+N)=-t;
101                     A(j,j-N)=-t;
102
103         end
104 end
105
106 %Next we include superconductivity.
107 %This loop will create particles at site specified in loop with both spin
        up and down,
108 %with coupling factor s. and annihilate correspondingly with coupling
        factor p:
109 if d==1
110 for i=1:N*N
111     A(i,3*N*N+i)=-s;
112     A(i+N*N,2*N*N+i)=+s;
113     A(i+3*N*N,i)=-p;
114     A(i+2*N*N,i+N*N)=+p;
115 end
116 else
117 for i=1:N*N
118     A(i,3*N*N+i)=-s_1(i);
119     A(i+N*N,2*N*N+i)=+s_1(i);
120     A(i+3*N*N,i)=-p_1(i);
121     A(i+2*N*N,i+N*N)=+p_1(i);
122    end
123 end
124
125 %(1,4) quadrant:
126 for i=1:N*N
127     for j=1:N*N
128         A(i+N*N,j+N*N)=A(i,j);
129     end
130 end
131 %for the 4'th quadrant:
132 for i=1:2*N*N
133     for j=1:2*N*N
134         A(i+2*N*N,j+2*N*N)=-A(j,i);
135     end
136 end
137
138 for i=1:2*N*N
139     A(i,i)=A(i,i)-u;
140     A(i+2*N*N,i+2*N*N)=A(i+2*N*N,i+2*N*N)+u;
141 end
142
143 %Numerical eigenvalues:
```

```
144
145 [Ve,E]=eig(A);
146 Ve=round(Ve,12);
147 E=round(eig(A),6);
148
149 %Now is an example of calculating the electron density expectation value
150
151 n1=zeros(1,4*N^2);
152 for f=1:N^2
153     for n=1:N^2
154         n1(n)=(fd(E(n)))*abs(Ve(f,n))^2;      %1st term spin up
155         n1(n+N^2)=(fd(E(n+N^2)))*abs(Ve(f,n+N^2))^2;      %2nd term spin up
156         n1(n+2*N^2)=(fd(E(n+2*N^2)))*abs(Ve(f,n+2*N^2))^2;
157         n1(n+3*N^2)=(fd(E(n+3*N^2)))*abs(Ve(f,n+3*N^2))^2;
158
159         n2(n)=(fd(E(n)))*abs(Ve(f+N^2,n))^2;      %1st term spin up
160         n2(n+N^2)=(fd(E(n+N^2)))*abs(Ve(f+N^2,n+N^2))^2;      %2nd term spin
              up
161         n2(n+2*N^2)=(fd(E(n+2*N^2)))*abs(Ve(f+N^2,n+2*N^2))^2;
162         n2(n+3*N^2)=(fd(E(n+3*N^2)))*abs(Ve(f+N^2,n+3*N^2))^2;
163     end
164 n_u(f)=sum(n1,2);
165 n_d(f)=sum(n2,2);
166 end
167
168 [M,I]=min(n_u);
169
170 if n_u(I)==0.5
171     break
172 end
173 if n_u(I)~=0.5
174     u=u-1/2*(n_u(I)-0.5);
175 end
176 end
177
178 %Implementing self consistency in the superconducting gap:
179
180 s_1=zeros(1,N^2);
181 for f=1:N^2
182     d1=zeros(1,4*N^2);
183     for n=1:N^2
184         d1(n)=fd(E(n))*conj(Ve(f+3*N^2,n))*Ve(f,n);
185         d1(n+N^2)=fd(E(n+N^2))*conj(Ve(f+3*N^2,n+N^2))*Ve(f,n+N^2);
186         d1(n+2*N^2)=fd(E(n+2*N^2))*conj(Ve(f+3*N^2,n+2*N^2))*Ve(f,n+2*N^2);
187         d1(n+3*N^2)=fd(E(n+3*N^2))*conj(Ve(f+3*N^2,n+3*N^2))*Ve(f,n+3*N^2);
188     end
189     s_1(f)=Vsc*sum(d1);
190     s1(d)=abs(s_1(1));
191 end
192 p_1=conj(s_1);
193 end
```